Study of *Helicobacter pylori* and SARS- CoV-2 Co-infection in Colon Cell Line- HT-29

M.Sc. Thesis

By

AKRATI TANDON

DEPARTMENT OF BIOSCIENCES AND BIOMEDICAL ENGINEERING

INDIAN INSTITUTE OF TECHNOLOGY INDORE

MAY 2023

Study of *Helicobacter pylori* and SARS- CoV-2 Co-infection in Colon Cell Line- HT-29

A THESIS

Submitted in partial fulfillment of the
requirements for the award of the degree
of
Master of Science

By

Akrati Tandon

DEPARTMENT OF BIOSCIENCES AND BIOMEDICAL ENGINEERING

INDIAN INSTITUTE OF TECHNOLOGY INDORE

MAY 2023

INDIAN INSTITUTE OF TECHNOLOGY INDORE

CANDIDATE'S DECLARATION

I hereby certify that the work which is being presented in the thesis entitled **Study of *Helicobacter pylori* and SARS-CoV-2 Co-infection in Colon cell line- HT-29** in the partial fulfillment of the requirements for the award of the degree of **MASTER OF SCIENCE IN BIOTECHNOLOGY** and submitted in the **DEPARTMENT OF BIOSCIENCES AND BIOMEDICAL ENGINEERING, Indian Institute of Technology Indore**, is an authentic record of my own work carried out during the time period from August 2021 to May 2023 under the supervision of Dr. Hem Chandra Jha, Associate Professor, IIT Indore.

The matter presented in this thesis has not been submitted by me for the award of any other degree of this or any other institute.

Akrati Tandon 23/5/23

Signature of the student
(Akrati Tandon)

This is to certify that the above statement made by the candidate is correct to the best of my/our knowledge.

24/5/2023

Signature of the Supervisor
(Dr. Hem Chandra Jha)

Akrati Tandon has successfully given his/her M.Sc. Oral Examination held on **May 8, 2023**.

24/5/2023

Signature of Supervisor of MSc thesis
Date:

P.V. Kodgire
Convener, DPGC
Date: 23/05/23

G.S.N. Murthy

Signature of PSPC Member
(Prof. Ganti S Murthy)
Date:

P.V. Kodgire
Signature of PSPC Member
(Prof. Prashant Kodgire)
Date: 23/05/23

ACKNOWLEDGEMENTS

I would like to express my gratitude to everyone who helped and supported me throughout my dissertation work. I especially want to thank my thesis supervisor, **Dr. Hem Chandra Jha, Associate Professor, Department of Biosciences and Biomedical Engineering,** who has guided me constantly throughout the project. I feel grateful for getting his constructive criticism, constant support, and inspirational words to keep my project going.

I sincerely thank our HoD, **Dr. Amit Kumar** and **PSPC** members **Prof. Ganti S. Murthy and Prof. Prashant Kodgire.**

I am immensely grateful to my seniors and lab members who have provided support in every possible manner for my growth. A special thanks to **Mr. Budhadev Baral** for his friendly support and encouragement at every step in my project. This project would not have been complete without your encouragement.

My greatest acknowledgement to my father **Mr. Ashutosh Tandon** and my mother **Mrs. Sonali Tandon** for their blessings, continuous encouragement and emotional support throughout my project duration. A special thanks to my sister, **Lavanya Tandon**.

I am grateful to my M.Sc. labmates, Sonali Adhikari, Samiksha Rele, Sidharth Singh and Priyanka Patra for being there always with me.

I would like to thank Sophisticated Instrument Facility (SIC) IIT Indore for the perfect logistic support and guidance they have extended to me. I am grateful to all the other staff of the Department of BSBE, IIT Indore and the institute library for their timely help.

Akrati Tandon

Dedicated to my parents,
sister, and friends, for their
unconditional support, faith
and blessings

ABSTRACT

The Severe Acute Respiratory syndrome coronavirus 2 (SARS-CoV-2), a novel β-coronavirus, is the main pathogenic agent of the rapidly spreading pandemic called coronavirus disease 2019 (COVID-19). Despite the pneumonia-like viral symptoms including cough, fever, sore throat, many hospitalized patients reported gastrointestinal (GI) symptoms like diarrhoea, abdominal pain, anorexia, vomiting as side-effect of viral infection. Researchers link these symptoms to co-infection of SARS-CoV-2 virus with gut microbiome, leading to gut dysbiosis. Thus, microbial co-infection in gut augment the infection cycle of the virus and the occurrence, development and symptoms of COVID-19. Our work aims to decipher the molecular mechanism involved in the severity posed by co-infection of gut pathogens and SARS-CoV-2. We have used colon carcinoma cell line HT-29 in our study. The results show increase in the inflammatory molecules at transcript and protein level. Further investigation of cell death pathways reveal a necrosis like cell death in the co-infected cells. Study of apoptotic and necrotic markers (Caspase-3, Caspase-8 and RIP-1) shows incease in the level of necroptotic marker RIP-1 in the co-infected cells. The infection and co-infection also damage the mitochondria in the HT-29 cells. Our study show the possible mechanism involved in co-infection mediated severity in colon cells.

Keywords: SARS-CoV-2, *Helicobacter pylori*, co-infection, inflammation, mitochondrial dysfunction, necroptosis

LIST OF PUBLICATIONS

1. **Tandon, A.**, Baral, B., Jha, H.C. (2023). The Role of Gut Microbial Co-infection in Augmenting the Severity of SARS-CoV-2: Insights from Molecular Mechanism of Co-infection in Colon Carcinoma Cell Line HT-29 (Manuscript under preparation)

2. **Tandon, A.**, Jha, H.C. (2023). Influence of Anti-hypertensive drugs consumption on the aggressiveness of COVID-19 disease in BP patients (Manuscript under preparation)

3. Baral, B., Saini, S., **Tandon, A.**, Singh, S., Rele, S., Jha, H.C. (2023) SARS-CoV-2 Envelope protein induces necroptosis and mediates inflammatory response in lung and colon cells through Receptor Interacting Kinase 1 (Manuscript under preparation)

4. Baral, B., Saini, S., Rele, S., Tambat, N., Singh, S., **Tandon, A.**, Tambat, P., and Jha, H.C. (2023) Anti-inflammatory and ROS scavenging activity of cannabis sativa leaf extract in bacterial and viral exposed lung and neural cells (Manuscript under preparation)

TABLE OF CONTENTS

LIST OF FIGURES

LIST OF TABLES

NOMENCLATURE

E. coli	*Escherichia coli*
H. pylori	*Helicobacter pylori*
SARS-CoV-2	Severe Acute Respiratory Syndrome Coronavirus-2
B.1.1.7	Alpha variant of SARS-CoV-2
B.1.351	Beta variant of SARS-CoV-2
P.1	Gamma variant of SARS-CoV-2
B.1.617.2	Delta variant of SARS-CoV-2
nCoV-2	Novel Coronavirus

ACRONYMS

ACE2	Angiotensin-Converting Enzyme 2
cDMEM	Complete Dulbecco Modified Eagle's Media
cDNA	Complimentary DNA
COVID-19	Coronavirus Disease 2019
DAPI	4′,6-diamidino-2-phenylindole
EB/AO	Ethidium Bromide/Acridine Orange
EDTA	Ethylenediaminetetraacetic acid
GAPDH	Glyceraldehyde 3-phosphate dehydrogenase
GI	Gastro-Intestinal
hpt	Hours Post Transfection
mRNA	Messenger ribonucleic acid
NF-κB	Nuclear Factor-kappa B
IL	Interleukins
ml	milliliter
mM	millimolar
qRT-PCR	Quantitative Real-Time PCR
RNA	Ribonucleic acid
RT-PCR	Real Time-Polymerase Chain Reaction
ssRNA	single stranded RNA
TLR2	Toll-like Receptor 2
TMPRSS2	transmembrane serine protease 2
TNFα	Tumor necrosis factor α
μL	microliter
μM	micro-molar
WHO	World Health Organization
°C	degree centigrade

CHAPTER 1: INTRODUCTION

1.1 SARS-CoV-2 – The contagious virus behind the COVID-19 disease

The initial cases of severe acute respiratory syndrome coronavirus 2 (SARS-CoV-2) infection appeared in December 2019 in Hubei province, China. Since then, it became a global threat and led to the lockdown throughout countries [1]. WHO estimates suggest the total number of global deaths attributable to the COVID-19 pandemic to be at least 3 million in 2020 [2]. Scientifically speaking, SARS-CoV-2 is a positive-sense ssRNA virus of genome size ~30kb [3]. This virus is infamously known to release its viral genome into human host cells by attaching its spike protein to host cell's membrane protein ACE2 [4]. Further fusion of viral and host membrane facilitates the entry of its' viral RNA to the host cell. This mechanism helps virus to infect cells and replicate its viral protein, thus stimulating the generation of new virus particles [5]. This virus commonly infected the lungs of patients, with common symptoms like cough, myalgias, and headache. In worst case scenario, caused pneumonia, severe respiratory distress syndrome, Acute respiratory failure, and multi-organ failure [6].

1.2 VOCs (Variant of Concerns) – The WHO terminology for the SARS-CoV-2

In nature, viruses continuously evolve as changes in the genetic code keeps on getting incorporated (caused by genetic mutations or viral recombination) during replication of the viral genome. Similarly,

SARS-CoV-2 has been known to develop persistent mutations, which led to variations that differ from those seen in the wild type strain of nCoV-2 [7]. During the pandemic, many variants of n-CoV2 were identified worldwide. WHO labeled a variant as VOC on basis of certain attributes including, increased transmissibility, severe disease and increased hospitalizations, reduced effectiveness of vaccines or prevailing treatments. The 5 VOCs which were first entitled with this status were – Alpha (B.1.1.7), Beta (B.1.351), Gamma (P.1), Delta (B.1.617.2), Omicron (B.1.1.529). Other VOCs including iota, kappa, epsilon, eta, zeta came much later [8].

1.3 Entry of SARS-CoV-2 to different organs

When researchers identified angiotensin-converting enzyme 2 (ACE2), a metallopeptidase as the functional receptor for SARS-CoV-2, they went on to understand the other route of this virus' entry to human body. Apart from lungs, ACE2 receptors are widely expressed in all other major organs of human body including heart, brain, blood vessels, kidney and GI tract organs like esophagus, stomach, gallbladder, colon, small intestine [9].

Other known receptors for SARS-CoV-2 binding includes TMPRSS2, CD147, Furin, etc. [10]. With ACE 2 being the most commonly found receptor in lung epithelial cells and gastro-enteric cells, researchers believe both respiratory and gut, as the entry modes for the virus [11]. Understanding the route of virus fusion and entry by GI cells will help us better understand the pathogenesis of the main disease manifestations in gut.

1.4 COVID-19 RNA in stool sample – Does SARS-CoV-2 enters GI tract?

During COVID-19, hospitalized patients reported GI related symptoms like abdominal pain, diarrhea, nausea, vomiting, anorexia etc. [12], [13]. Moreover, viral RNA was detected in 82% stool sample of COVID-19 positive patients when RT-PCR was performed on oropharyngeal swabs, stool, urine samples of approximately 300 patients [12], [14].

Within GI tract, mucosa-associated lymphoid tissue (MALT) forms the I line of defense and is involved in inducing immune response on microbe exposure [15]. Studies suggest that these GI related symptoms might be related to gut dysbiosis caused by SARS-CoV-2 infection in GI tract [16]. Moreover, it was found that the SARS-CoV-2 virus penetrates the cell by binding its S-protein to the human ACE2 receptor, which, in particular, is widely expressed by intestinal enterocytes and colon cells. Thus, SARS-CoV-2 spike is one of the important structural proteins of the virus which contributes to its disease pathogenesis [17], [18].

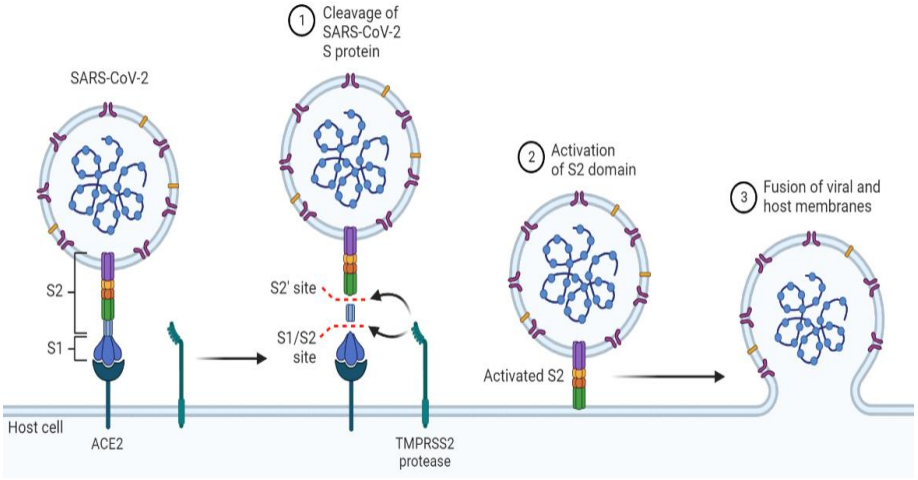

Figure 1.1 **Spike binds to ACE2 receptors and TMPRSS2 receptors (made with Biorender)**

These studies lead to the possibility that SARS-CoV-2 virus enters the gut cells and creates an imbalance in the gut microenvironment [19]. This further might lead to imbalances in the niche of gut-inhabited microbes thus, causing an increase in number of microbes not good for our digestive system and simultaneous decrease in the number of good bacteria.

1.5 *Helicobacter pylori* and gut dysbiosis

One of the pathogenic bacteria found in gut is *H. pylori,* as it resides in more than 50% of world population [20]. *Helicobacter pylori* (*H. pylori*) is a group I carcinogen, which causes gastric cancer by inducing DNA damage in gastric cells [18], [21]. Infection of *H. pylori* causes acute-chronic inflammation which further alters the various cellular processes like genomic stability, cell cycle, apoptosis, autophagy, and antioxidant defense [22]. This bacteria's life cycle involves release of toxins, and inflammation in the gastric cells. Naturally, it does not harm the gut, but external factors like viral infection, bacterial infection or other stimulants manifest a disbalance in the colony of gut-residing *H. pylori* [23]. This leads to gut dysbiosis and might cause an elevated negative effect of foreign pathogenic species for instance, SARS-CoV-2 in the human gut.

1.6 Co-infection of SARS-CoV-2 and *H. pylori*

The presence of viral genome of SARS-CoV-2 virus in COVID-19 patients even after the qRT-PCR of respiratory sample is negative, clearly indicates that the virus infects the gastro-intestinal tract as well [14].

Upon infection, both *H. pylori* and SARS-CoV-2 induces an inflammatory pathway. Having being colonized in human gut for

more than 60,000 years, *H. pylori* has evolved itself to create a favorable niche for itself [24]. *H. pylori* is also a commensal bacterium, which provides protective effect to IBD patients by downregulating pro-inflammatory cytokines and chemokines [25]. In general, *H. pylori* is associated and have been reported widely to cause hyper-inflammatory diseases including peptic ulcers, gastritis, and colon cancer [26], [27].

Thus, it can be hypothesized that SARS-CoV-2 infection in GI associated cells induces an inflammatory response which might influence the inflammatory reaction induced by the already present *H. pylori* bacteria.

For in vitro experiments involving the study of co-infection, the concentration of plasmid (WT and Delta) at which the expression of genes will be optimum needs to be analyzed. Further, prime inflammatory markers including IL-6, TNFα, IL-10 profiles need to be assessed by performing these experiments. Such studies hold relevance as co-infection raises the difficulty of diagnosis, treatment and might lead to more severity of disease pathology [28].

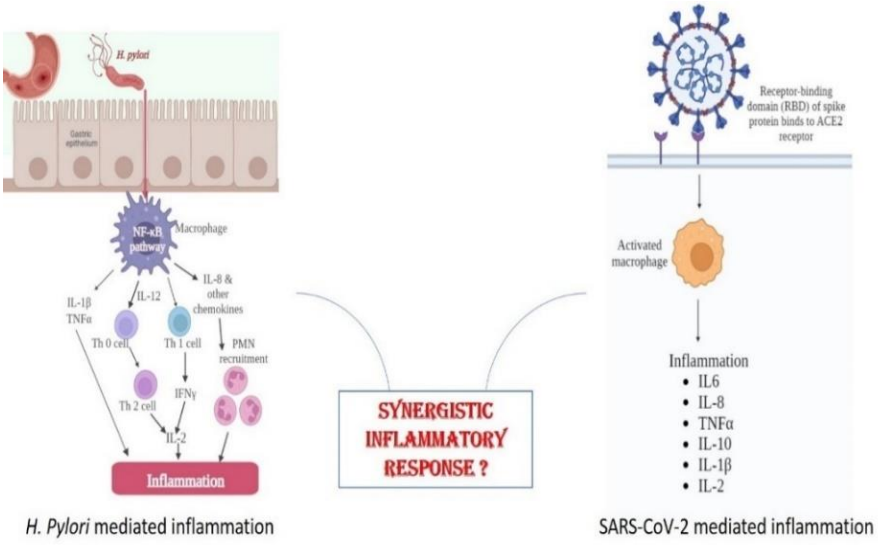

Figure 1.2 **Hypothesis of co-infection study (Made with Biorender)**

One of the inflammatory pathways that is common between *H. pylori* and SARS-CoV-2 infection is the NF-κB pathway. The Spike protein of SARS virus binds to ACE2 receptors which further interacts with TLR2 protein in cell to induce NF-κB mediated inflammatory response [29]. Similarly, *H. pylori* mediates its inflammatory response through NF-κB pathway by binding to TLR2 receptors [30]–[32].

Hence, there is a possibility that co-infection of SARS-CoV-2 in pre-infected colon cells with *H. pylori* bacteria can cause elevated inflammatory response. This hyperinflammation can be a possible reason for observed gastro-intestinal physiological symptoms in COVID-19 patients.

Thus, co-infection study by modelling a natural scenario can help understand the pathway and altered inflammasome in the colon microenvironment.

1.7 The hypothesized Co-infection Model

To conduct our study, we had to devise a model which incorporates both, single infection of SARS-CoV-2 and *H. pylori* as well as the co-infection of both SARS-CoV-2 and *H. pylori*.

As found out by dose optimization experiments, we kept the time-point for incubating Delta-transfected cells to be 48 hpt. This time-point was kept constant for coinfected samples as well.

For *H. pylori* infection, 24 hpi was the time-point for incubation of single infection samples, i.e., HB1 and HJ9. This is because, the bacteria take minimum of 12 hours to establish its infection in the cells.

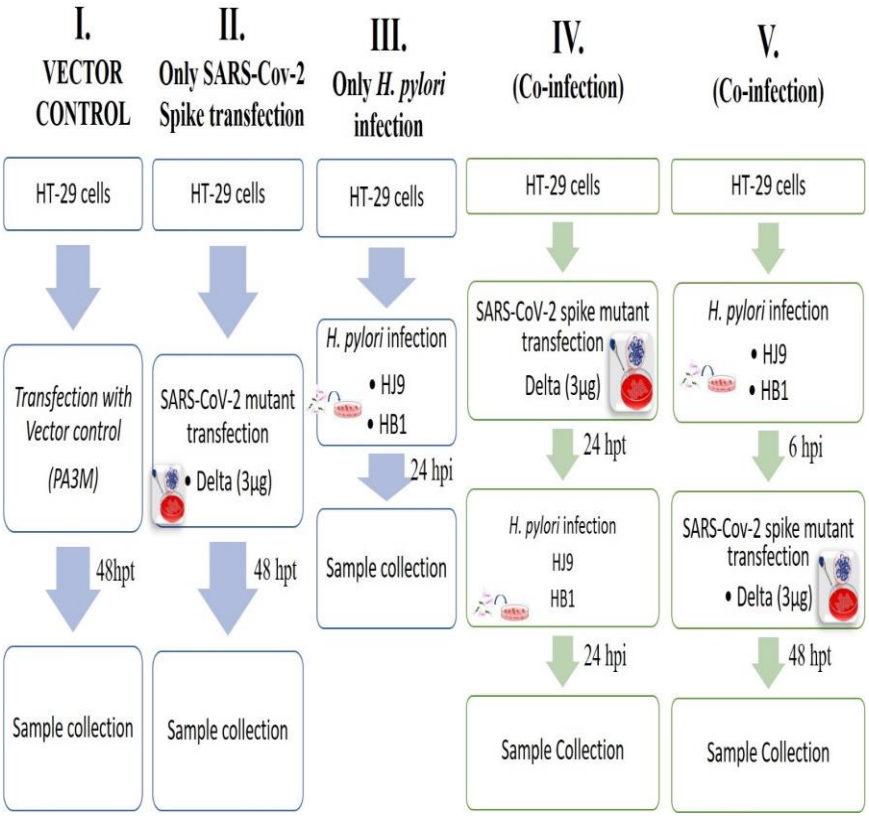

Figure 1.3 **Experimental setup for co-infection study of *H. pylori* and SARS-CoV-2**

For infection in Sample III, IV and V, HB1 and HJ9 were used to infect the HT-29 cells at MOI = 100. After 24 hours of incubation, sample III i. e. HB1 infected HT-29 cells and HJ9 infected HT-29 cells were collected for further experiments. For sample IV i. e. transfection with Delta plasmid followed by infection with HB1 and transfection with Delta plasmid followed by infection with HJ9, samples were collected after 48 hours post transfection. For sample V, i. e. infection with HB1 followed by transfection with Delta plasmid and infection with HJ9 followed by transfection with Delta plasmid, the samples were collected after 54 hours post infection.

1.8 Cell death and associated pathological symptoms

The most reported GI-related pathological symptoms in COVID-19 disease were abdominal pain, diarrhea [12], [33]. At the cellular level, entry of SARS-CoV-2 and its effective replication causes in enteric cells causes a pathogenic load and leads to activation of cell death pathways. Some researchers also hypothesize that SARS-CoV-2 modulates the apoptosis signaling pathway, more of like hijacking the natural system of cell, to induce cell death [34]. It is known that SARS-CoV-2 infection triggers apoptosis through caspase-8 activation, which is extrinsic pathway of cell death [35]. This route of cell death also involves mitochondria to release pro-apoptotic factors.

CHAPTER 2: REVIEW OF PAST WORK

The etiology of COVID-19 is commonly associated with a hyperinflammatory response [36]. The researchers are still finding out the precise mechanism of SARS-CoV-2- induced inflammation. The spike protein of this virus has highest binding affinity for ACE2 receptors [37]. When spike protein binds to the ACE2 receptors, a potent inflammatory response is induced. The cytokine storm includes upregulation of cytokines including IL-6, IL-1β, TNFα, CXCL1, CXCL2, and CCL2 [38]. The most commonly reported being IL-6, TNFα. Several biochemical studies have revealed that the spike protein can induce inflammation by triggering the activation of the NF-κB pathway in a manner that relies on MyD88, an adaptor protein . [29]. Very interestingly, recent findings demonstrate that the spike protein elicits an inflammatory response by engaging the NF-κB pathway through a mechanism dependent on TLR-2. [39]–[41].

Another inflammatory molecule, TNFα has been found to be highly elevated in SARS-CoV-2 patients [42]. TNFα has also been known to activate the inactive form of NF-κB. The activated NF-κB acts as transcriptional factor and promotes transcription of inflammatory genes [22], [43], [44]. Thus, elevation of TNFα and NF-κB justifies the cytokine storm in COVID-19 patients.

Among all 3 waves of COVID-19, wave II saw most deaths due to cytokine storm in patients. In the same wave, gastrointestinal symptoms were reported most [45], [46]. This led to various questions wherein GI manifestation in COVID-19 was researched. Studies on this topic range from gut microbiome dysbiosis in COVID-19 to the complications in colon cancer patients due to nCoV-19 [16], [47], [48]. Among the bacterial microbiome, abdominal pain, and diarrhea in coronavirus disease-2019 patients has been strongly correlated to presence of *Helicobacter pylori* in

the gut [18], [49]. Studies suggest, it is the high expression of ACE 2 receptors in gut cells that aid binding and infection of SARS-CoV-2 virus [50], [51].

Similar to SARS-CoV-2, *H. pylori* also induces NF-κB mediated inflammation in gastric and colon cells [52], [53]. But on the other hand, it has also been found that *H. pylori* wants to survive the gastric niche, hence, it promotes release of anti-inflammatory cytokines and anti-apoptotic molecules [54], [55].

Therefore, a contrasting question arises, if co-infection of *H. pylori* and SARS-CoV-2 in gastric cells, will induce inflammation and cell death, or will be directed towards pro-survival pathways.

Another contrasting question that arises is, if cell death occurs, then viral replication will get limited as number of cells for infection will also be limited. Also, if excessive cell death occurs, this will lead to inflammation and tissue damage, the hallmarks of severe COVID-19.

Hence, this remains to be elucidated what major inflammatory and cell-death pathways will be significantly activated or altered if the coinfection of gut bacteria, *H. pylori* and virus, SARS-CoV-2 occurs in the gut.

CHAPTER 3: AIMS AND OBJECTIVE

3.1 – To find out the optimized concentration of spike plasmid for our experiments.

3.2 – To understand the inflammasome associated with co-infection of SARS-CoV-2 and *Helicobacter pylori*.

3.3 – To understand if mitochondrial dysfunction is associated with the cell death.

3.4 – To find out the type of cell death associated with co-infection of SARS-CoV-2 and *Helicobacter pylori*.

CHAPTER 4: MATERIALS AND METHODS

4.1 Material

4.1.1 For Lab Procedures

- Laminar airflow hood (for working on bacteria)
- Centrifuge
- Refrigerator (-80 °C, -20 °C, 0 °C, 4 °C)
- Heat block
- pH meter
- Gel documentation system
- Incubator shaker
- Vortex shaker
- Pipette with tips
- Serological pipettes
- Gel electrophoretic kit
- 15 ml screw-cap centrifuge tubes
- 50 ml screw-cap centrifuge tubes
- 1.5 ml microcentrifuge tubes
- LB Agar plates
- LB media
- 0.7% Agarose gel
- Biosafety cabinet (cell culture)
- Culture plate (100mm, 60mm, 6-well)
- PCR thermal cycler
- Real-Time PCR System (Agilent AriaMx)
- CO_2 incubator
- Liquid Nitrogen Container
- Steripipette
- cell lifter

4.1.2 Chemicals for Midiprep

- Solution I: 50 mM glucose, 10 mM EDTA and 25 mM Tris-HCl, pH 8.0
- Solution II: 0.2 N NaOH, 1% SDS
- Solution III: 3 M potassium acetate, 2 M acetic acid
- RNase A
- Phenol
- Phenol: Chloroform ::1:1
- Chloroform:Isoamylalcohol::24:1
- Isopropanol
- Sodium Acetate
- 70% Ethanol
- Autoclaved Water

4.1.3 Requirements for Dose Optimization

- Plasmids (pcDNA 3.1 Myc tag (PA3M), pcDNA 3.1 SARS-CoV-2 spike WT (Wuhan Strain), pcDNA 3.3 SARS-CoV-2 spike Delta)
- Invitrogen Lipofectamine transfection reagent (P3000, Lipofectamine)
- Trizol for RNA isolation
- RT-PCR (SyBR green, spike primer (FP and RP), GAPDH primer mix (FP and RP))
- HT-29 cells (loaded in 60 mm plate) with 80% confluency
- cDMEM, plain DMEM
- Trypsin 0.25% v/v
- PBS (Phosphate Buffer Saline)

4.1.4 Requirements for Co-infection Model Sample preparation

- Plasmids (pcDNA 3.1 Myc tag (PA3M), pcDNA 3.3 SARS-CoV-2 spike Delta)
- *H. pylori* strain – HB1, HJ9
- Invitrogen Lipofectamine transfection reagent (P3000, Lipofectamine)
- Trizol for RNA isolation
- RT-PCR (SyBR green, primer mix (FP and RP))
- HT-29 cells (loaded in 60mm plate) with 70% confluency
- cDMEM, plain DMEM

4.2 Methods

4.2.1 Cell line

HT-29 cells were obtained from the National Centre for Cell Science, India. The cells were cultured in Dulbecco's modified Eagle's medium (DMEM; Thermo Scientific, USA) supplemented with 10% Fetal Bovine Serum (FBS; Thermo Scientific, USA), 50 U/ml penicillin, 100 µg/ml streptomycin, in a humidified atmosphere with 5% CO_2 at 37 °C i.e., inside incubator situated in cell culture unit. For splitting the cells, 0.25% Trypsin was used each time.

4.2.2 *Helicobacter pylori* and their culture

For infection of cells with *Helicobacter pylori*, bacteria were obtained originally from the biopsy and juice samples of suspected gastritis patients of Choithram Hospital, Indore. Clinical samples were isolated by lab seniors and, further, named serially by them.

For this study, we used HB1 strain, obtained from the biopsy sample of the patient, and HJ9, obtained from the juice sample of the patient. The glycerol stock made by lab seniors was used to revive each strain of *Helicobacter pylori.* BHI Agar plates were streaked with glycerol stock, and incubated in a microaerophilic chamber (Whitley DG 250) containing specific growth conditions (i.e., 85% N_2, 10% CO_2 and 5% O_2) at 37 ℃. Then, a single colony was picked from the Columbia agar plate of each sample and inoculated in complete brain heart infusion media (BHI, Cat. No. 237500- BD Brain Heart Infusion broth), containing 10% Fetal Bovine Serum (FBS Hi-media, Cat. No. RM-10432) with 3X *H. pylori* selective antibiotics (5 mg/L cefsulodin, 10 mg/L vancomycin, 5 mg/L amphotericin B, 5 mg/L trimethoprim) in a snap cap tube (BD, Cat. No. 352001) [56].

4.2.3 Transformation of pcDNA 3.3-SARS-CoV-2 spike WT and Mutant strains in Competent cells *E. coli* DH5α

1. Competent cells were taken out from -80 ℃ and placed immediately on ice to thaw the cells.
2. >100 ng of plasmid DNA was added to 50 µl of competent cells aliquot, and the bottom of the tube was gently flicked.
3. Cells were incubated for 10-15’ on an ice bath.
4. A heat shock of 90 seconds was performed at 42 ℃.
5. 100 µl fresh LB broth was added to the transformed cells.
6. These cells were placed on ice for 3-5’.
7. Transformed cells were kept on an orbital shaker for 50-55’ at 37 ℃ (330 rpm).
8. 200 µl competent cells were plated on LB agar (Amp+) and were kept in incubator.

9. After 12–14 hours, LB plate with the colony of transformed cells was taken out for further use.

4.2.4 Midiprep technique for plasmid isolation

1. A single colony was picked from LB plate with transformed *E. coli* cells and, inoculated in 3 ml LB culture with 1x Ampicillin.
2. After 10–12 hours incubation at 220 rpm, 1 ml culture was inoculated into 100 ml LB media containing 100 µl Ampicillin.
3. The inoculated culture media was kept in a shaker incubator overnight at 220 rpm.
4. This culture was poured into a 50 ml centrifuge tube and centrifuged at 3000 rpm for 10'.
5. After centrifugation, the cell pellet was washed with 10 ml PBS and centrifuged at 3000 rpm for 5'.
6. 10 ml solution I was added to 100 ml culture and incubated on ice for 10'.
7. 20 ml solution II was added to 100 ml culture and incubated on ice for 10', meanwhile the tube was gently mixed in between.
8. 15 ml solution III was added to 100 ml culture and incubated on ice for 10'. Like the previous step, the tube was gently mixed in between.
9. The tube containing pelleted cells with all three solutions was centrifuged at 5000 rpm for 25'. After the centrifugation, the supernatant was sieved with kimwipe.
10. Further, 45µl of 30µg/ml RNaseA solution was added and kept for incubation at 42 °C for 1 hour.
11. Then, an equi-volume phenol was added to the solution, kept at RT for 10' and centrifuged at 5000 rpm for 25'.

12. The supernatant was carefully transferred to new tube and an equi-volume Phenol: Chloroform (1:1) mixture was added to the solution, kept at RT for 10', and centrifuged again at 5000 rpm for 25'.
13. The supernatant was again carefully transferred to new tube and an equi-volume Chloroform: Isoamyl alcohol solution (24:1) was added to the solution, kept at RT for 10' and centrifuged at 5000 rpm for 25'.
14. The supernatant was carefully transferred to a new tube and 2x volume of 100% isopropanol and 10% Sodium acetate was added. This solution mixture was stored at -80 ℃ overnight.
15. The next day, the plasmid-containing solution was spun down at 5000 rpm for 25' at 40 ℃, and the supernatant was carefully removed and the remaining pellet was washed with 70% ethanol.
16. This solution was centrifuged at 5000 rpm for 25' at 40 ℃. The supernatant was discarded, and the pellet was air-dried for 15' The pellet was then dissolved in 100 µl autoclaved water.
17. Nanodrop reading was taken, and samples were loaded on 0.7% agarose gel in TAE.

4.2.5 Transfection of HT-29 cells with plasmid

1. For transfecting HT-29 cells with spike plasmid at 3 µg concentration (optimized dose through experiments), 6 µl of plasmid (500 ng/µl) was mixed with P3000 (Invitrogen Lipofectamine™ 3000 Transfection Reagent) and DMEM. This mixture was labelled as Tube-1 and was kept for incubation for 20'.
2. In Tube- 2, DMEM and Lipofectamine reagent (Invitrogen Lipofectamine™ 3000 Transfection Reagent) were added, and this solution was incubated for 20'.
3. After incubation of both Tube-1 and Tube-2 individually, both the tubes were mixed and incubated for another 20'.

4. After incubation, the desired volume of this transfection mixture was added to the culture plates and swirled in rotational motion for 30 sec - 1'.
5. Further, the cell culture plates were incubated for desired time points [57].

4.2.6 RNA Isolation

1. 300 µl Trizol was added to each cell pellet, and the mixture was thoroughly mixed by vortexing to ensure homogenization and efficient cell lysis.
2. Following a 5' incubation period, the lysate is transferred into a microcentrifuge tube (MCT). This is to ensure that the lysate is maintained in a small, contained space, making it easier to carry out subsequent steps in the protocol.
3. Next, 100 µl chloroform was added to the MCT and mixed gently by inverting several times to enable effective separation of the aqueous phase from organic phase.
4. The MCT was then left to incubate at room temperature for 3'. After incubation, the MCT was centrifuged at 12,000 g for 15'. This step was crucial for separating the different phases of the lysate.
5. Once the centrifugation was complete, the aqueous phase was carefully transferred to a fresh tube. To the aqueous phase, 250 µl of isopropanol was added to initiate RNA precipitation.
6. The RNA was allowed to precipitate for 10', after which the tube was centrifuged at 12,000 g for 15' to obtain the RNA pellet. This pellet contained the isolated RNA.
7. The RNA pellet was then washed with 500 µl of 75% ethanol, and the tube was incubated for 5'. The ethanol was essential for

washing away any residual contaminants that may have co-pelleted with the RNA.

8. The tube was then centrifuged at 8,000 g for 8’ to pellet the RNA once again. This step was essential for further compacting the RNA pellet and removing any remaining ethanol.
9. The RNA pellet was then air-dried for 10’ to remove any residual ethanol completely and 20 µl of autoclaved water was added, and the mixture was gently mixed to resuspend the RNA. Nanodrop reading was taken to check concentration and purity of RNA [58].

4.2.7 cDNA Synthesis

1. From the isolated RNA, dilutions were prepared so that final concentration was in the range of 1-2.5 µg in 10 µl solution.
2. Master mix I, containing Random hexamer, dNTPs were added to each RNA sample and the mixture was incubated on a heat block at 65 °C for 5’.
3. Master mix II containing 5x buffer, RNase inhibitor, and autoclaved double distilled water was prepared.
4. For RNA concentration 1-2 µg, 0.5 µl Reverse transcriptase was added and for >2 µg RNA, 1 µl Reverse transcriptase was added to Master mix II.
5. After incubation on heat block, 7 µl of Master mix II and Reverse transcriptase was added to each RNA sample.
6. These prepared samples were kept for Takara cDNA Synthesis Protocol in thermal cycler.

Table 1: Stages of cDNA preparation in thermocycler

STAGE-1	STAGE-2	STAGE-3	
30 °C, 10’	42 °C, 60’	70 °C, 15’	4 °C, ∞

4.2.8 qRT-PCR

cDNA was subjected to qRT-PCR using SyBR green real-time master mix (Thermo Scientific, USA) on Agilent AriaMX, following the instrument standard cycling conditions. The primers used for qRT-PCR are listed in Appendix. The relative gene expression of the target genes was analysed using the $2^{-\Delta\Delta Ct}$ method. Briefly, delta Ct ($^{\Delta Ct}$) is the difference obtained after subtracting the cycle threshold (Ct) value of the gene of interest and GAPDH. Further, delta delta Ct ($^{\Delta\Delta Ct}$) is the difference between the delta Ct ($^{\Delta Ct}$) of the sample (D1/3) after infection/transfection and the control sample (D0). These values are finally used to calculate the fold change. All reactions were performed in triplicate and repeated at least twice.

Table 2: Stages of qRT-PCR cycle in AriaMX Thermocycler

HOT-START	DENATURATION	ANNEALING	EXTENSION
95 °C, 10’	95 °C, 15 sec	58.5 °C, 20 sec	72 °C, 20 sec
1 cycle	40 cycles		

4.2.9 Western Blot

1. The cells upon infection/transfection, according to the co-infection model, were collected by scraping with cell lifter, washed with ice-cold PBS.
2. Cells were lysed in radioimmunoprecipitation assay (RIPA) buffer [10 mM Tris (pH 7.5), 150 mM sodium chloride, 2 mM EDTA, 1% NP-40] containing protease and phosphatase inhibitors. Proteins in

the supernatant were quantified using Bradford protein assay reagents (Pierce, Rockford, IL).

3. Equal quantities of protein from each group were separated using SDS-PAGE and transferred onto 0.45 μm PVDF membranes (Millipore, Billerica, MA).
4. Membranes were blocked with 4.5% BSA and incubated with primary antibodies specifically used for the study for 12 hours at 4 °C.
5. Following incubation and washing with TBST, the membrane was treated with 1:3000 dilution of horseradish peroxidase-conjugated anti-rabbit/mouse antibodies for 1 hour at room temperature.
6. The chemiluminescent detection was based on the Pierce ECL Western blotting substrate (Thermo Scientific, Rockford, IL). Image analysis and quantification was performed using Image J software (National Institutes of Health, Bethesda, MA, USA).

4.2.10 EB/AO Staining

1. For differentiation of cells based on live, apoptotic, and necrotic, dual acridine orange (AO): ethidium bromide (EB) (Sigma-Aldrich, St. Louis, MO, USA) staining was carried out. For AO: EB staining, cells were seeded to a final concentration of 0.1×10^6 in a 12-well plate.
2. At the time-point of experiment, cells were washed gently with PBS. These cells were then stained with 200 μL of dual fluorescent staining solution containing 100 μg/ml of AO and EB each (AO/EB, Sigma, St. Louis, MO).
3. 5’ post-incubation at 37 °C, cells were imaged using Olympus IX83 fluorescence microscope using 480 and 535 nm excitation filters.

The images of cells upon AO: EB staining was obtained after two biological repeats of the experiment. Furthermore, the percent cell population of early and late apoptotic cells, necrotic cells was calculated and subsequently plotted for each experiment.

4.2.11 Immunofluorescence

1. The expression of genes of interest (spike, RIP1, ß- catenin and c-myc) in response to co-infection were analysed using immunofluorescence assay. 0.5 x 10^6 cells were seeded onto coverslips and infected/transfected at respective time-points according to the co-infection model.
2. At the time-point of experiment, cells were fixed with 4% paraformaldehyde.
3. The cells were permeabilized using freshly prepared 0.2% Triton X100 for 20-40 min.
4. Blocking was performed using 1% BSA (Sigma, St. Louis, MO) followed by incubation with primary antibodies (anti- spike antibody, 1:50 dilution, anti- RIP antibody, 1:250 dilution, anti- ß-catenin, 1:100 dilution and anti- c-myc, 1:300 dilution) for 2 hours at room temperature.
5. HT-29 cells were then washed and incubated with a secondary antibody (1:1000 dilution) conjugated with different fluorophores and DAPI solution.
6. The coverslips were transferred onto a small drop of antifade mounting medium
7. Slides were observed under CLSM (FluoView 1000, Olympus America Inc., USA).

Image analysis and quantification measurements were performed using Image J software (National Institutes of Health, Bethesda,

MA, USA). The fluorescence intensity was calculated and plotted in comparison to the uninfected control of the respective groups.

4.2.12 Mitotracker Red and Green Assay

1. After completion of the infection or treatment period cells were treated with (200 nM) of Mito tracker red in 500 μL of plain DMEM incubated for 40 min at 37 °C.
2. After incubation cells were washed with PBS, followed by treatment of (100 nM) Mito tracker green in 500 μL of serum-free media for 40 min.
3. After completion of the incubation period cells were washed again with PBS and images were taken under Olympus IX83 fluorescent microscope aided with cell Sens imaging software at 20× objective magnification [59]

4.2.13 Statistical analysis

All the in vitro experiments were performed in triplicates. Data throughout the thesis project were represented as means ± errors of means (SEM) of two independent experiments. A 2-tailed T-test was performed to compare differences in the mean values for every data obtained through different experiments. p-values of 2-tailed student's t-test was performed to evaluate the significance of differences in the mean values. The significance test was calculated taking Vector Control (VC) as reference. p-values of <0.05, <0.01 and < 0.001 were considered statistically significant and represented with *, ** and ***, respectively

CHAPTER 5: RESULTS AND DISCUSSION

5.1 PLASMID ISOLATION AND TRANSFECTION DOSE OPTIMIZATION FOR pcDNA 3.3 SPIKE IN HT-29 CELLS

5.1.1 Transformation of *E. coli* and Plasmid isolation

Transformed *E. coli* cells were streaked and midiprep technique was performed for plasmid isolation at high volume.

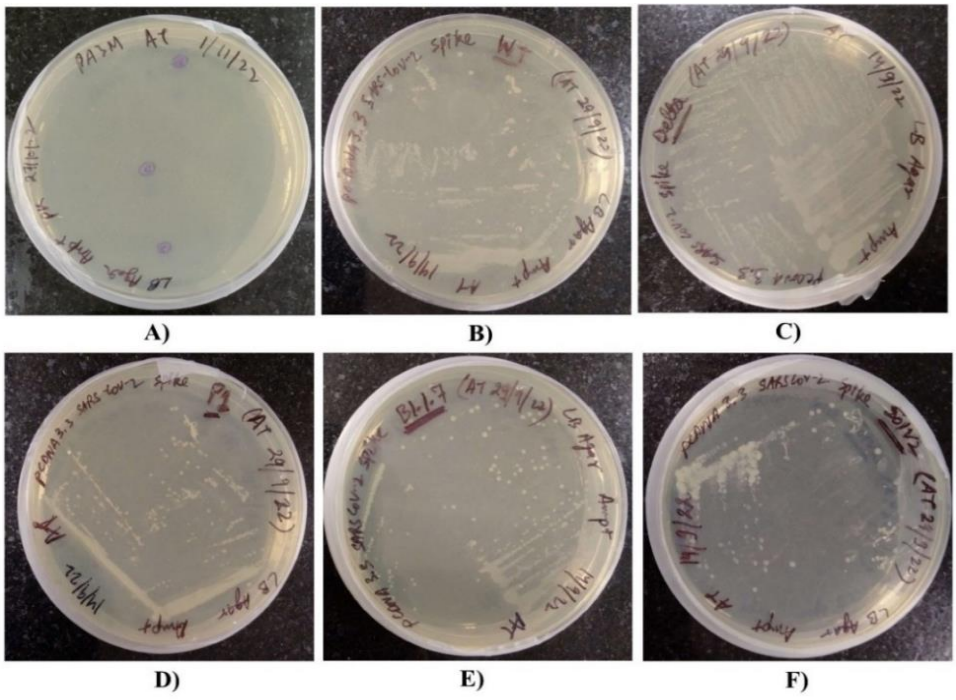

Figure 5.1 **Transformation of *E. coli* DH5α with plasmid.** A) PA3M (pcDNA 3.1 myc tag), pcDNA 3.3 SARS-CoV-2 Spike variants- {B) Wild Type, C) Delta (B1.317.2), D) Gamma(P1), E) Alpha (B1.1.7), F) Beta (501V2)} strain.

A)

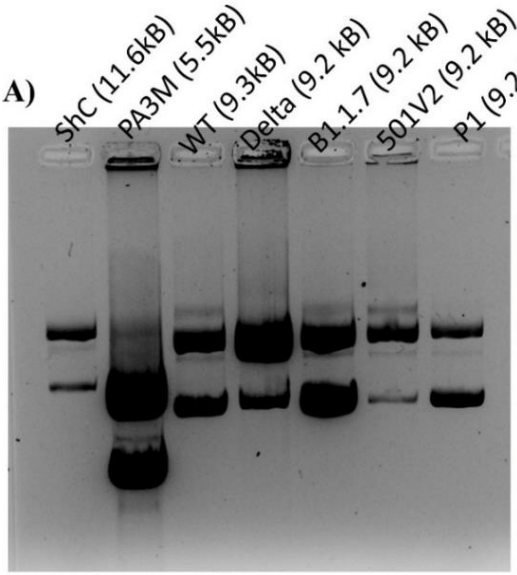

B)

pcDNA 3.3-SARS-CoV-2 spike	Plasmid Concentration (ng/µL)
PA3M	2380
WT	1760
Delta	1000
B1.1.7	2200
501V2	2700
P1	2794

Figure 5.2 **Isolated plasmid concentration and gel.** A) Gel image for isolated plasmid through Midiprep - ShC, PA3M, pcDNA 3.3 SARS-CoV-2 spike WT, Delta, B1.1.7, 501V2 and P1 strain. The plasmid was separated using 0.7% Agarose gel. B) Concentration of isolated plasmid estimated through UV-Vis spectrophotometer at 260 nm.

5.1.2 Dose optimization of plasmid in HT-29 cells

To find out the exact concentration/dose of plasmid for achieving optimum expression of spike gene in HT-29 cells, dose optimization was performed using qRT- PCR. Use of optimum dose ensures that our protein of interest gets expressed without causing any toxicity in cells. For this, we took 3 different concentrations (as shown in Table 5.1) of pcDNA 3.3 SARS-CoV-2 Delta plasmid and transfected the HT-29 cells with PA3M as control vector. Apart from dose optimization, optimum time for incubation of cells was also estimated by taking 3 different time points – 24, 36 and 48 hpt.

The following table represents the different concentration of spike plasmid used for transfection.

Table 5.1: Different plasmid concentrations for transfection in HT-29

pcDNA 3.1 SARS- CoV-2 Myc	**3**	**2**	**1**	**0**
pcDNA 3.3 SARS-CoV-2 spike Delta	**0**	**1**	**2**	**3**

At transcript level, pcDNA 3.3 SARS-CoV-2 delta plasmid shows significant expression at 3 µg in HT-29 cells at 48 hpt. Moreover, at this concentration and time-point, the morphology of cells remained intact. Though, at 24 hpt, mRNA level of spike gene was also significantly high, but for our study we chose 48 hpt as our incubation time. This is because spike is a viral protein and difficult to express in mammalian system, Hence, we wanted to ensure maximum transcript level, so that a substantial amount of protein is being expressed in our model cell line – HT-29. It was clearly observed that 2.5 µg concentration did not show any significant difference at all 3 time-points.

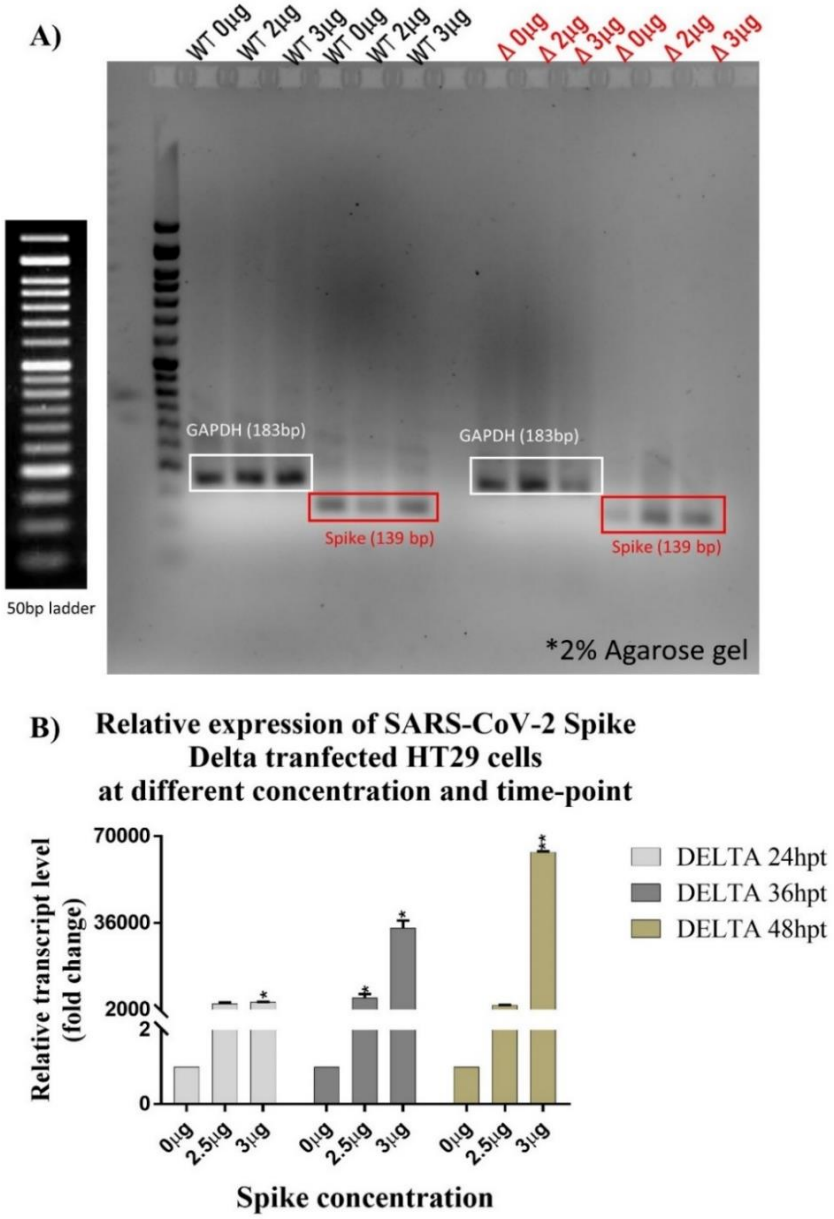

Figure 5.3 **qRT-PCR of Spike transfected HT-29 cells for dose optimization.** A) PCR amplification product of cDNA obtained from HT-29 cells transfected with pcDNA 3.1 SARS-CoV-2 WT and pcDNA 3.3 SARS-CoV-2 Delta (Genes – GAPDH, Spike) at 48 hpt. B) Graphical data representing fold change in RT-PCR products of HT-29 cells transfected with pcDNA 3.3 SARS-CoV-2 Delta (24, 36, 48 hpt). The graphs were plotted using ImageJ software and statistics was calculated using t -Test to check the significance level.

5.1.3 Expression of spike protein in transfected HT-29 cells

After confirming the expression of spike at mRNA level, next step was to check the expression of spike gene at protein level. This was important to know if our gene of interest was getting translated in cell model or not. For this, PA3M transfected and pcDNA 3.3 SARS-CoV-2 Delta transfected HT-29 cells were subjected to Immunofluorescence staining. The slides were observed at 100X under Confocal Microscope.

From the confocal imaging, a significant 16 times fold change in expression of spike protein with transfection conditions of 3 µg concentration and 48 hpt was observed. Thus, this experiment proved that our protein of interest, spike is getting transcribed as well as translated to its protein form.

These experiments which involved optimizing the dose and time-point for transfection in our cell line- HT-29 were important for our subsequent study. Further, we can visualize the various pathways, mediated by this protein in our model cell line.

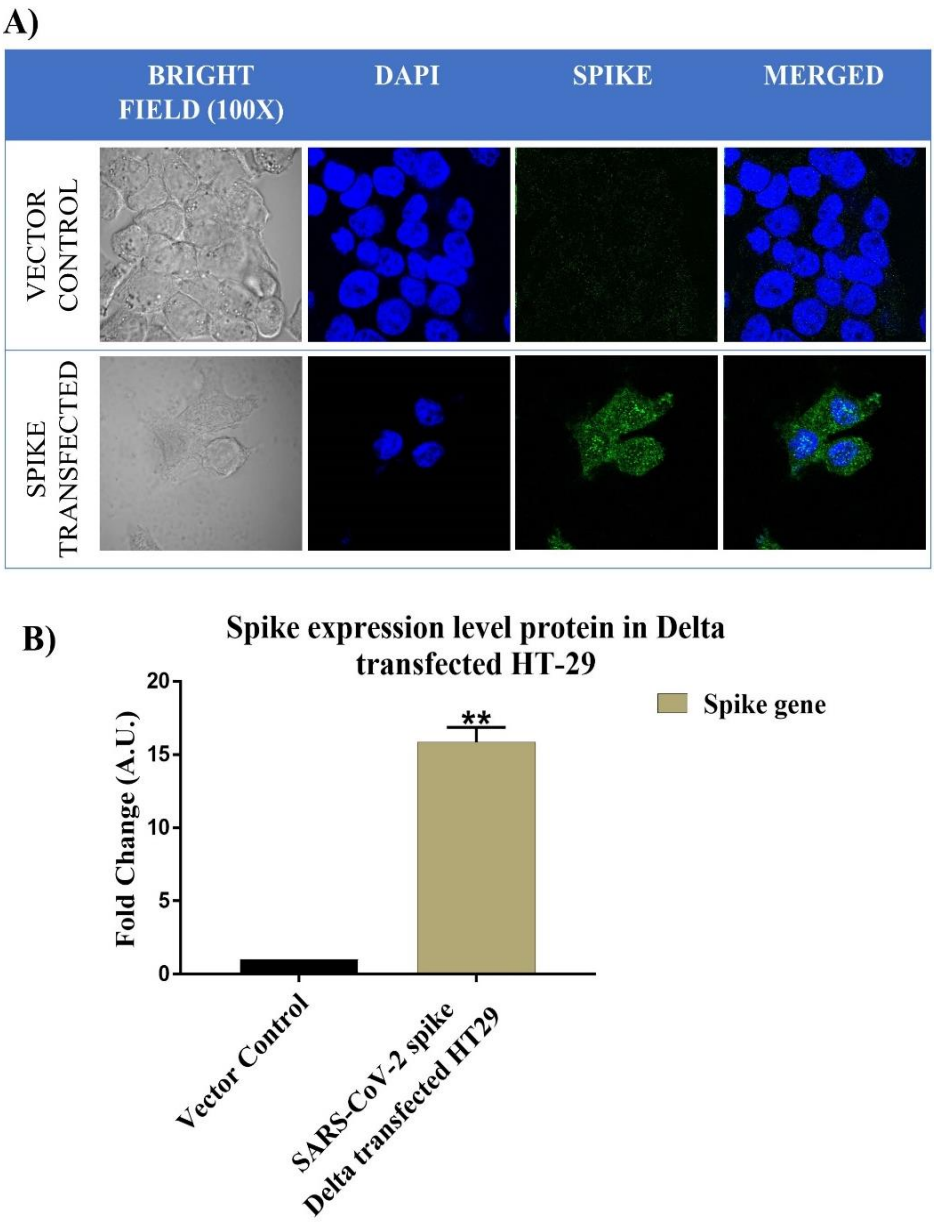

Figure 5.4 **Immunofluorescence of Spike transfected HT-29 cells at optimized dose.** A) Immunofluorescence image of spike gene in pcDNA 3.3 SARS-CoV-2 spike mutant Delta transfected HT-29 cells (48 hpt). B) Graphical representation of fold change in expression of spike gene (48 hpt) using ImageJ Software.

5.2 INFLAMMASOME STUDY IN CO-INFECTION MODEL OF *H. pylori* and SARS-CoV-2 IN COLON CELL LINE – HT-29

5.2.1 Significant Spike gene expression in co-infection samples versus individually infected samples

In the proposed co-infection model, before performing any study, it was important to check the expression level of spike gene. This helped us ensure that we were analyzing our experiments, keeping in mind, if co-infection causes any change in the expression of viral protein. Moreover, this helped us to gain understanding if the presence of *H. pylori* infection caused any difference in the expression of spike gene. For this, we performed qRT-PCR, using spike primer, of cell samples infected and collected according to the co-infection model.

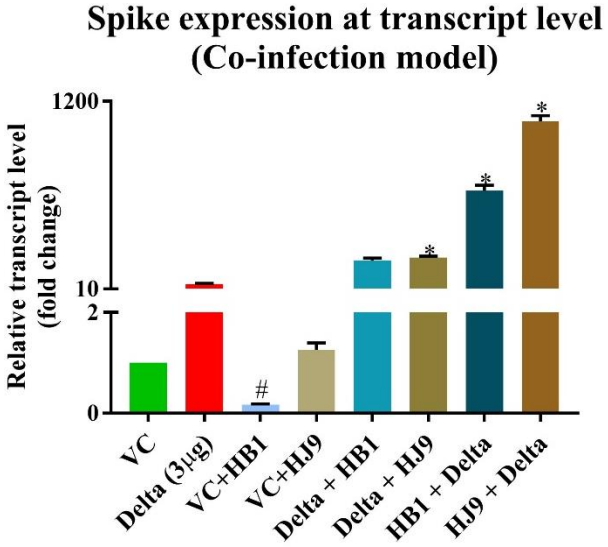

Figure 5.5 **Relative expression of the spike gene in pcDNA 3.3 SARS-CoV-2 spike mutant Delta transfected HT-29 cells analyzed using qRT – PCR.**

From the qRT- PCR result, an upregulation in spike gene at transcript level was observed in sample – HB1 + Delta and HJ9 + Delta. This result indicates that the model HB1 + Delta and HJ9 + Delta mimics the natural environment, wherein, bacteria already pre-colonize the colon. Moreover, a subsequent infection of SARS-CoV-2 virus in colon cells might lead to activation/alterations in different molecular pathways.

Further, we wanted to check if mRNA transcript of spike translates to protein in co-infection model, hence, we performed immunofluorescence staining of all samples of co-infection model using anti- spike antibody (CST, E7V3M) and the slides were examined under a confocal laser scanning microscope (CLSM) (FluoView 1000, Olympus America Inc., USA) using 480 and 535 nm excitation filters.

Interestingly, at protein level too, we did observe an increased expression of spike protein in co-infected samples as compared to single bacterial infection. But, in comparison to Delta transfected samples, we did not observe any significant fold change in protein, as was observed at transcript level.

This observation suggests that *H. pylori* infection and expression of bacterial genes might play a role in suppressing the expression of viral protein – spike at translational level. An alternate justification can be, that when bacteria infect a transfected cell, this might induce cell death in co-infected cells. Thus, leading to decreased expression of spike protein in cell population.

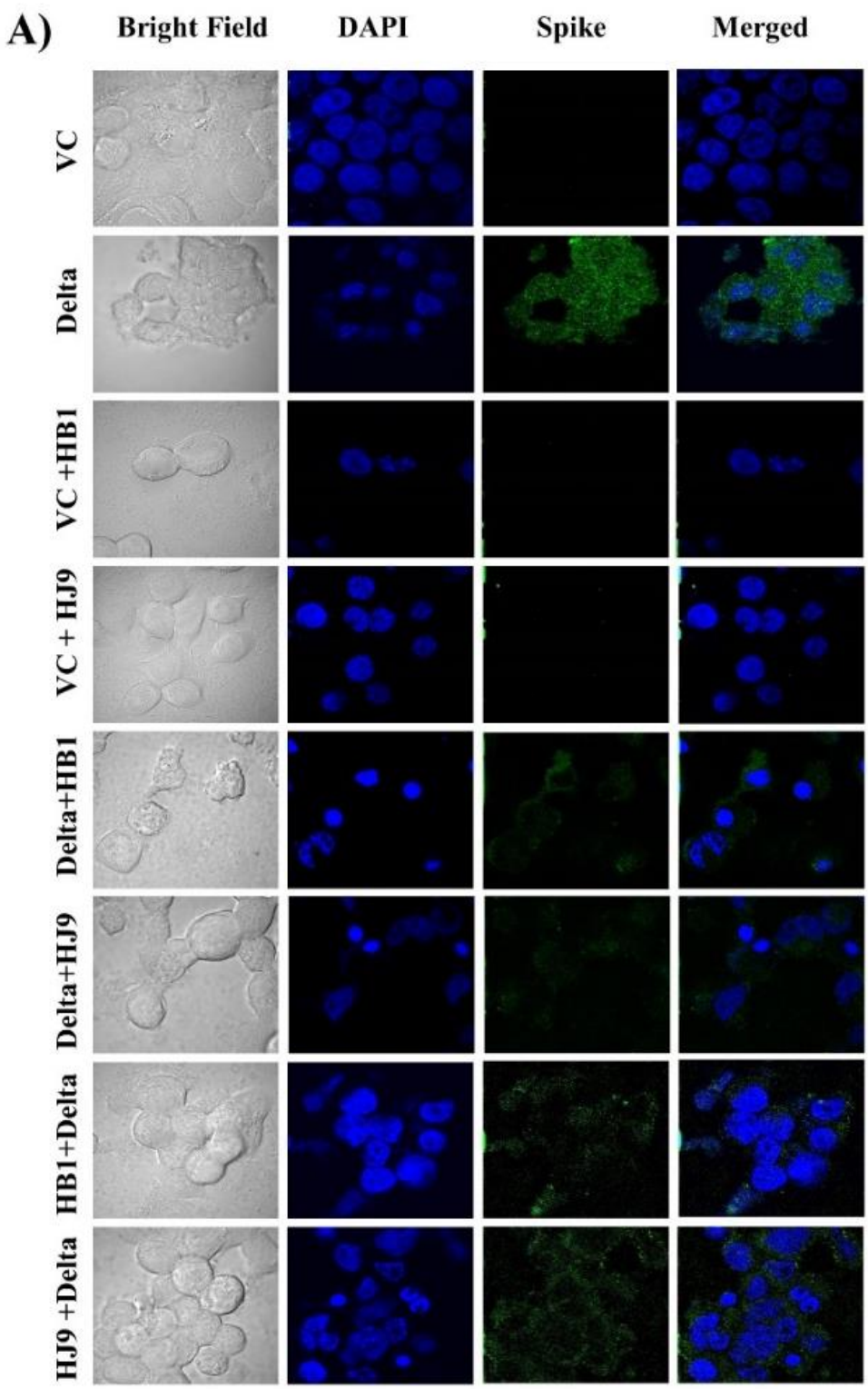
A)
Bright Field
DAPI
Spike
Merged
VC
Delta
VC +HB1
VC + HJ9
Delta+HB1
Delta+HJ9
HB1+Delta
HJ9 +Delta

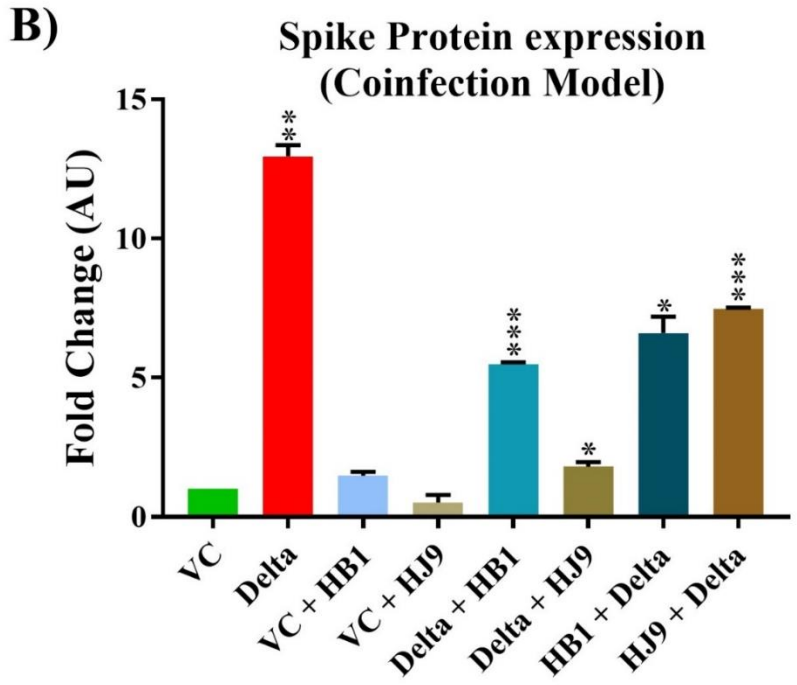

Figure 5.6 **Expression of Spike protein in HT-29 Co-infection Model.** A) The expression of spike protein in HT-29 cells, infected according to the co-infection model, was checked by Immunofluorescence assay. B) Graphical representation of quantified IF images through the Image J software. The statistical test was performed taking Vector Control (VC) as reference. p-values of <0.05, <0.01 and < 0.001 were considered statistically significant and represented with *, ** and ***, respectively.

5.2.2 Inflammasome study in Co-infection Model

To study the expression level of different inflammatory genes at transcript level, a connectome which linked the commonly known inflammatory pathways of *H. pylori* and SARS-CoV-2 were created using CytoScape software. The list included – IL-6, IL-10, IL-1ß, IFN-ß1, IFN-ß2, CXCL1, CXCL2, IFN-γ, TNFα.

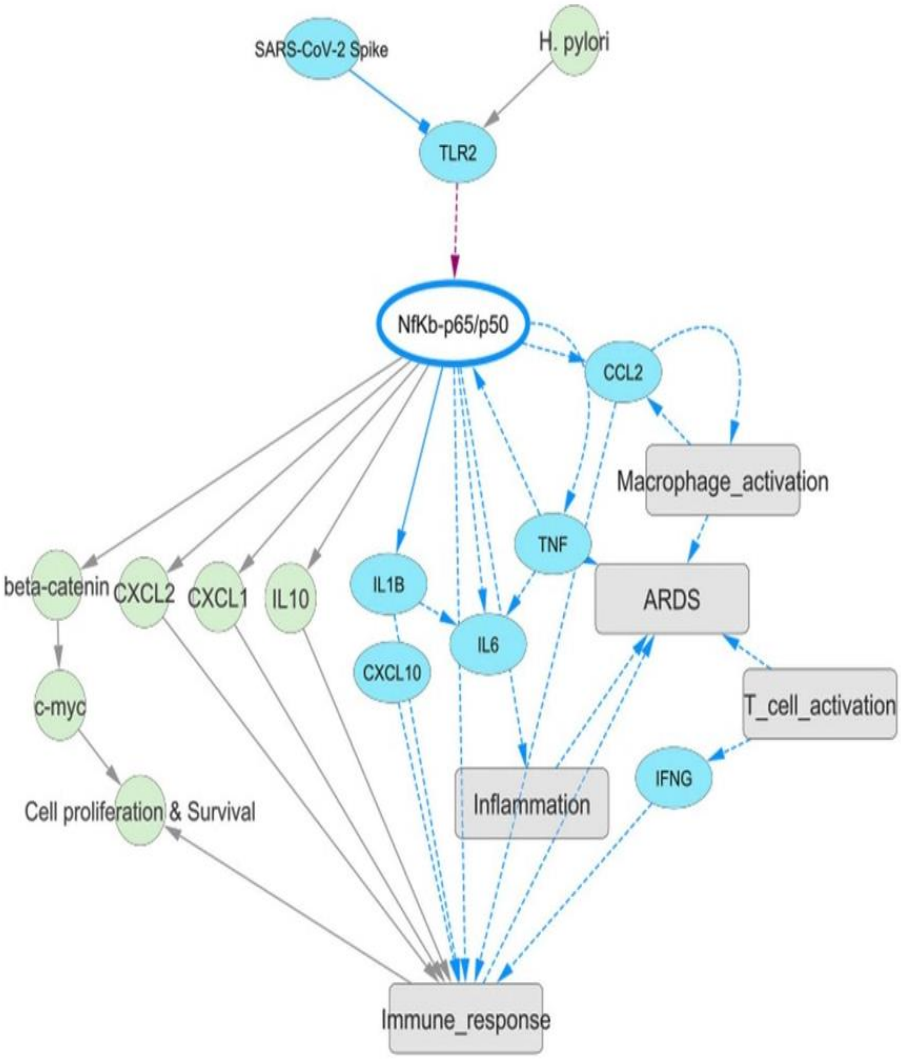

Figure 5.7 **Connectome network representing common pathway for SARS-CoV-2 infection and *H. pylori* infection.**

Since, a detailed understanding about any alterations in the inflammatory pathway occurring in co-infection samples, might help in understanding of overall changes in cell at pathological level. Hence, we wanted to check a few common inflammatory genes and NF-κB pathway, the common inflammatory pathway in SARS-CoV-2 and *H. pylori* infection.

First up, we performed qRT -PCR of these common genes to screen any significant changes in the expression of these genes due to co-infection.

Using the connectome designed using already available literature as reference, few of the inflammatory genes that were analyzed using qRT-PCR did show some intrigue pattern.

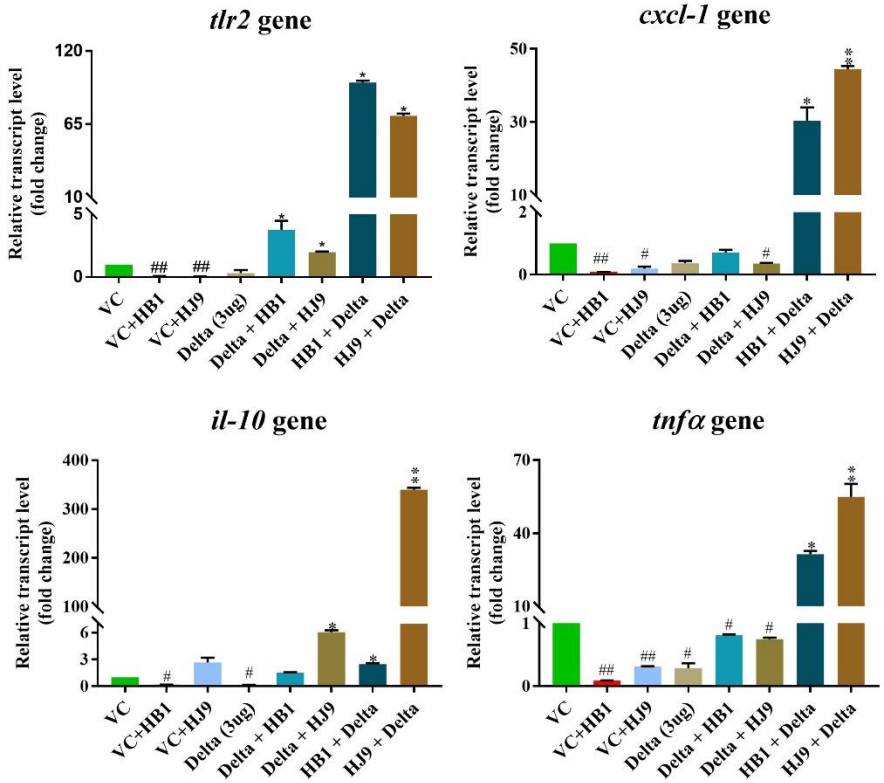

Figure 5.8 **Relative expression of Inflammatory genes mRNA in infected samples according to the co-infection model.** A statistical test for comparison of mean values was performed. p-values of <0.05, <0.01 and <0.001 were considered statistically significant and represented with #/*, ##/** and ###/***, denoting downregulation/upregulation respectively.

In co-infection sample, HB1 + Delta and HJ9 + Delta, where spike expression was significantly higher, the transcript level of *il-10, tnfα* and *cxcl1*, was found to be upregulated as compared to other samples. Interestingly, the level of *tlr2* was also higher in this co-infection model. This indicates that SARS-CoV-2 infection might be aggravated in colon cells pre-infected with *H. pylori* bacteria.

Among the inflammatory genes which showed any significant differences i. e. *il-10, cxcl1 and tnfα*, each one play an important role in inflammatory pathway. IL-10 is a cytokine known for its potent anti- inflammatory and immunosuppressive effects. In COVID-19, concurrently elevated IL-10 was commonly reported. This might suggest that IL-10 tries to mitigate the hyperinflammatory response due to infection by elevating its level of expression. Though, some studies also suggest the role of IL-10 as a pro-inflammatory cytokine in certain conditions. Another chemokine CXCL1, was found to be significantly upregulated. CXCL1 plays a pro-inflammatory role which recruit neutrophils through the PI3K / AKT pathway. TNFα, is another pro-inflammatory cytokine that was commonly found to be upregulated in COVID-19 patients. The same cytokine is also reported as one of the molecules upregulated significantly in *H. pylori* infection. As expected, our results show that the co-infection of *H. pylori* and SARS-CoV-2, induces significant inflammatory response involving TNFα as an important inflammatory marker.

Few studies suggest that SARS-CoV-2 mediated upregulation of TNFα, triggers cytokine release syndrome (CRS) and facilitates the interaction of SARS-CoV-2 virus with ACE2 receptors. At cellular level, TNF-a plays a significant role in activation of NF-κB mediated transcription of inflammatory cytokines.

To further unveil if the co-infection model of our study follows NF-κB inflammation pathway, we performed western blot of our co-infection model using Anti- NF-κB and Anti- ß-catenin antibodies.

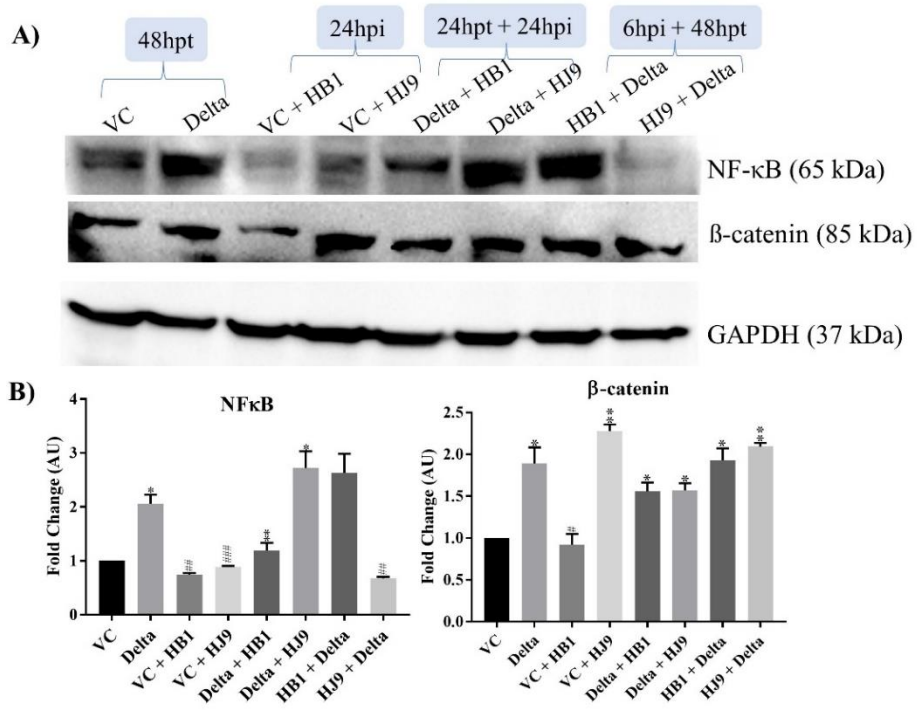

Figure 5.9 **Inflammasome study of co-infection model at protein level.** A) Co-infection of *H. pylori and* SARS-CoV-2 shows downregulation of NFkB as compared to Delta transfected sample, whereas, ß-catenin gets upregulated in co-infection sample as compared to Vector control and Delta transfected HT-29. B) Quantitative representation of Western blot image using Image J software and representative graph presented in terms of fold changes for single infection/transfection or co-infection. The significance test was calculated taking Vector Control (VC) as reference. p-values of <0.05, <0.01 and < 0.001 were considered statistically significant and represented with *, ** and ***, respectively.

NF-κB is found to be downregulated in HB1 + Delta and HJ9 + Delta co-infection samples. This result is in congruence as per previously reported finding by lab's senior colleagues that NF-κB expression is downregulated after 12 hours of *H. pylori* infection. Thus, at time point of 48 hours and 54 hours, NF-κB is downregulated. Further, ß-catenin, an apoptotic and inflammatory marker is upregulated in co-infection model. Since, ß-catenin is a known marker, expressed downstream to the NF-κB signalling pathway.

Hence, these results suggest that if co-infection occurs in a person, inflammatory response through NF-κB mediated pathway might be cause of disease symptoms.

To validate our finding, we further wanted to check the expression of c-myc, an inflammatory molecule downstream to the NF-κB and ß-catenin. For this, we performed the dual immunofluorescence staining of ß-catenin and c-myc stained green and red respectively. As expected, the expression of ß-catenin was upregulated in co-infected samples but, to our surprise c-myc also showed significant upregulation in the co-infected samples. Thus, this confirmed our hypothesis that co-infection of SARS-CoV-2 and *H. pylori* induces activation of NF-κB mediated inflammation.

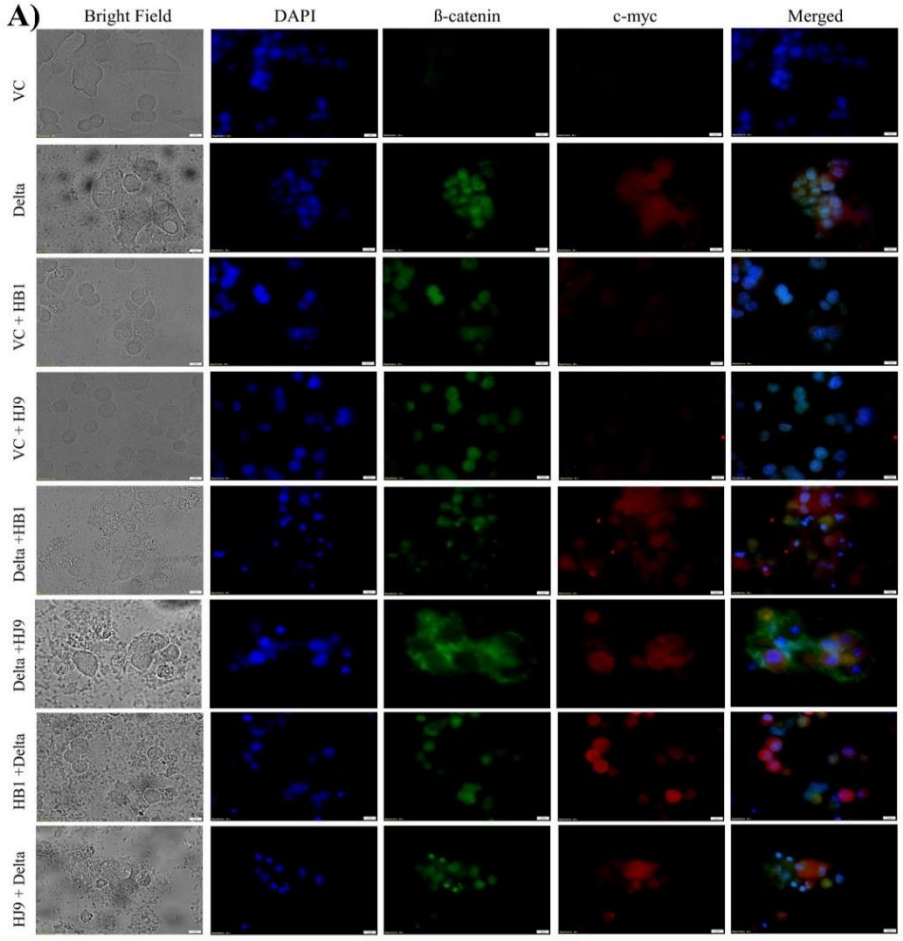

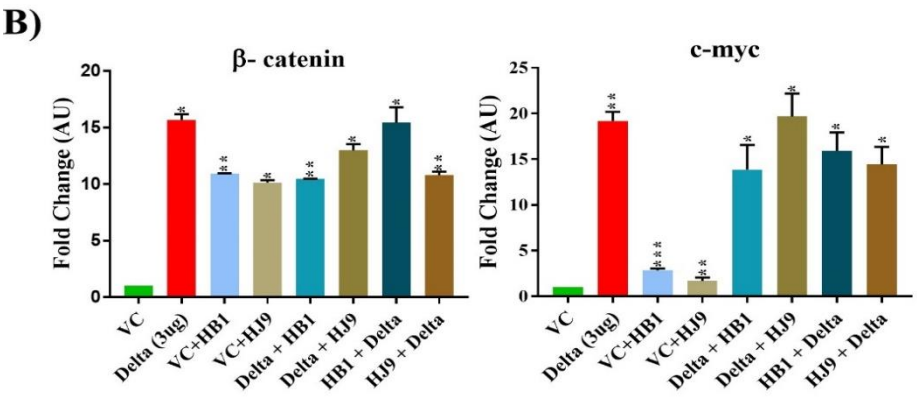

Figure 5.10 **Dual Immunofluorescence staining for ß-catenin and c-myc.** (A) Immunofluorescence assay of inflammatory markers ß- catenin and c-myc in *H. pylori* and pcDNA 3.3 SARS-CoV-2 spike co-infected HT-29 cells. (B) Quantitative representation of Western blot image using Image J software, $p < 0.05$; #/*, $p < 0.01$; ##/**, < 0.001; ###/***, were considered statistically significant.

5.3 MITOCHONDRIAL DYSFUNCTION STUDY

In general, viral infections affect the function of mitochondria in cells to impact the cell's metabolism. SARS-CoV-2 infection has been reported to cause mitochondrial damage through fragmentation and leaky membrane. As a result, the cytochrome c released from damaged mitochondria leads to activation of caspases. This marks the cell for apoptosis or programmed cell death.

For visualizing the mitochondrial condition and function, Mitotracker assay was performed. Mito tracker red was used to access the active mitochondria and its accumulation is dependent on mitochondrial membrane potential. Meanwhile, Mito tracker green binds to mitochondrial proteins regardless of their membrane potential and represents the mitochondrial mass.

The results of this assay suggest that both mitochondrial potential and mass are getting reduced in co-infected samples.

Reduction in mitochondrial mass and potential is a signal of bioenergetic stress in the cell and may lead to the release of apoptotic factors leading to

cell death. This indicates that apoptotic pathways might be activated in co-infection model.

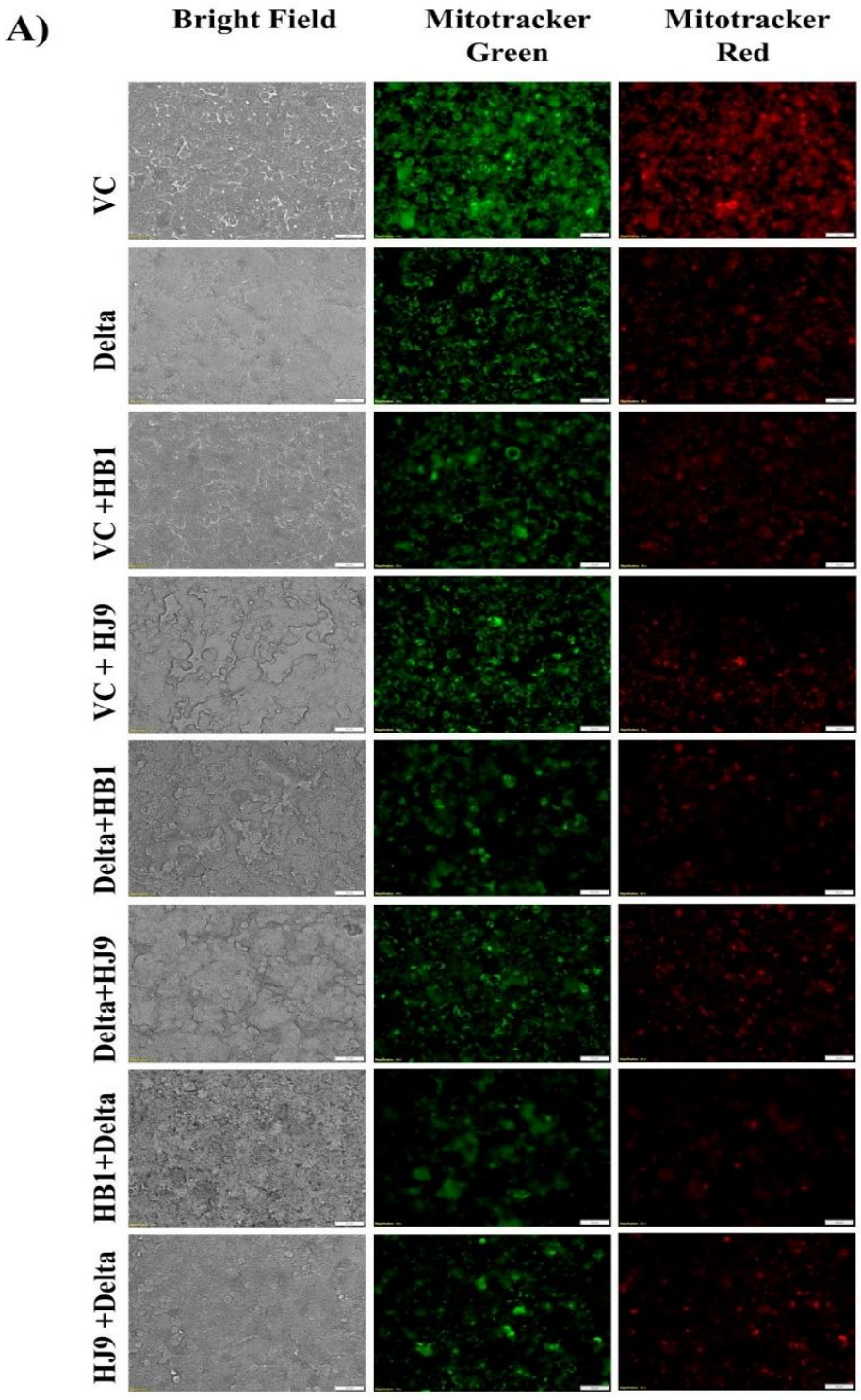

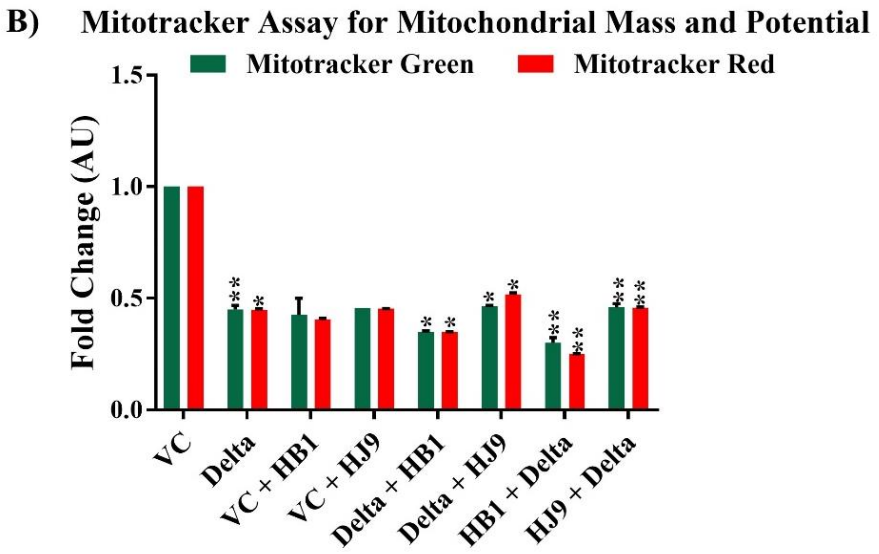

Figure 5.11 **Mitotracker assay to check mitochondrial damage in co-infection model.** A) Mitotracker Red and Green Assay representing the Membrane potential and mitochondrial mass in co-infection model respectively. B) Quantification of EB/AO stained HT-29 cells was performed using Image J software. $p < 0.5$ is significant.

5.4 STUDY OF CELL DEATH PATHWAY

5.4.1 Apoptotic gene expression in co-infection model

To check the level of apoptotic genes at transcript level, we performed RT-PCR and found a significant fold change in the death receptor – *fadd*, mitochondria related genes – *bak, bid*. Though there was a slight upregulation in *caspase 9*, but other genes in extrinsic pathway, including BAX did not show any significant changes. bcl_2, a marker involved in intrinsic cell death pathway showed upregulation in co-infected sample. Thus, this suggests that apoptosis in the co-infected cells can be attributed to activation of intrinsic pathway.

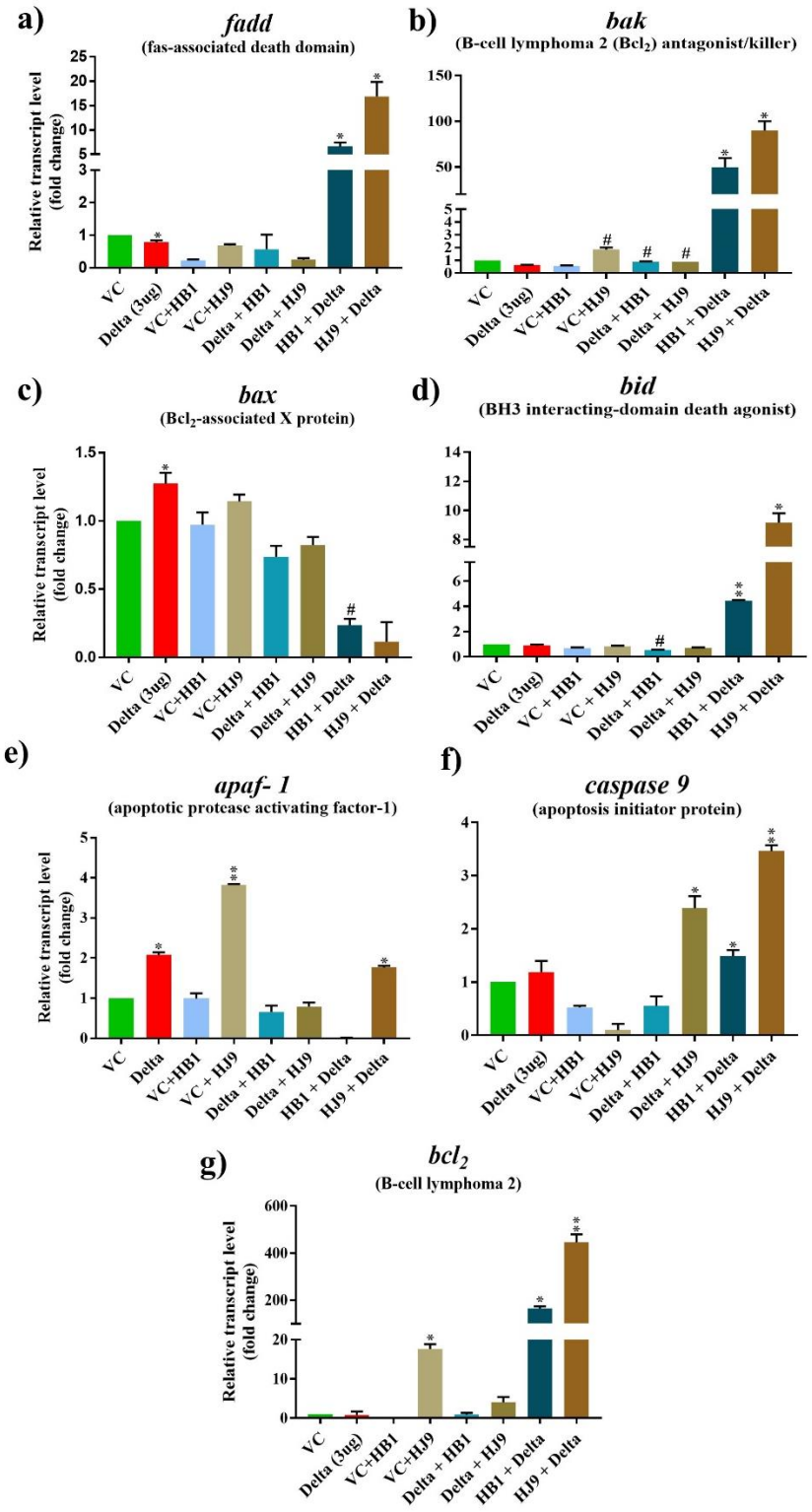

Figure 5.12 **qRT- PCR of apoptotic genes and genes regulating the production of chemical modulators (chemokines, cytokines) in HT-29 cells infected/transfected according to co-infection model.** The

significance test was calculated taking Vector Control (VC) as reference. p-values of <0.05, <0.01 and <0.001 were considered statistically significant and represented with #/*, ##/** and ###/***, denoting downregulation/upregulation respectively.

5.4.2 Intrinsic or extrinsic apoptosis pathway

Since, qRT-PCR results showed us that co-infection of SARS-CoV-2 and *H. pylori* increased the checked the markers of apoptosis – Caspase 8, a protein of extrinsic pathway and Caspase 3 – the executioner caspase. To our surprise, we did not find any significant fold change in the level of both the caspases. Also, we could not find if the apoptosis occurs through intrinsic or extrinsic pathway.

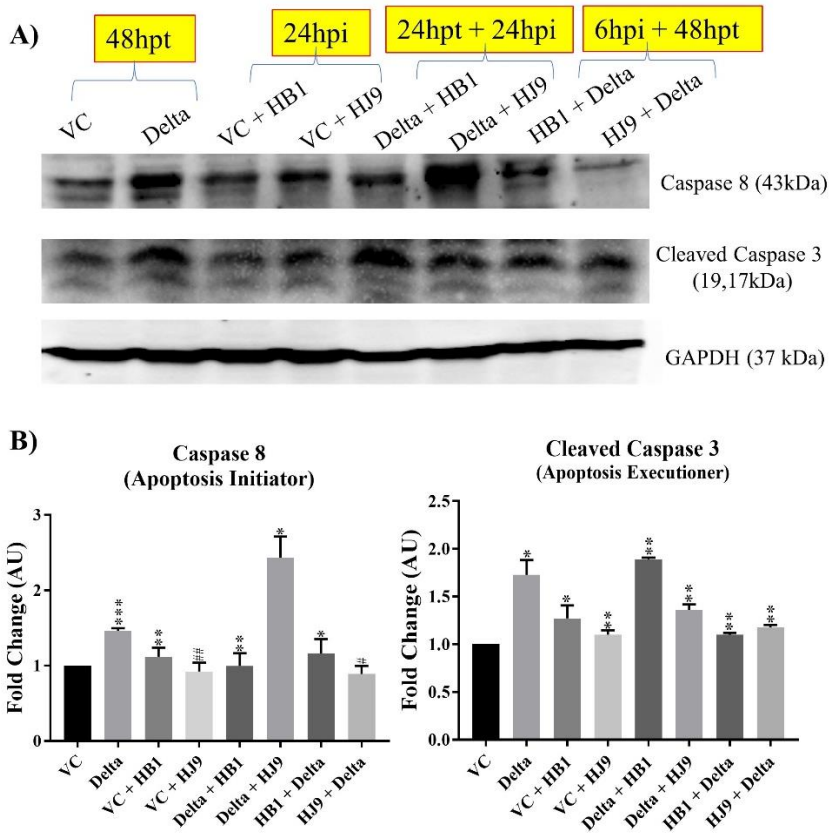

Figure 5.13 **Western blot analysis for initiator (Caspase 8) and executioner (Caspase 3) in co-infection model.** A) Co-infection of *H. pylori* and SARS-CoV-2 shows upregulation of caspase 8 in Delta + HJ9

sample as compared to Delta transfected sample, whereas, caspase 3 does not show any significant change in co-infection sample as compared to Vector control and Delta transfected HT-29. B) Quantitative representation of Western blot image using Image J software and representative graph presented in terms of fold changes for single infection/transfection or co-infection. The significance test was calculated taking Vector Control (VC) as reference. p-values of <0.05, <0.01 and < 0.001 were considered statistically significant and represented with *, ** and ***, respectively.

5.4.3 EB/AO Staining for cell death

In our co-infection model, we wanted to check the percentage of live and dead cells. For this, we performed EB/AO staining and analyzed the percentage of live and dead cells. Cells which were green represent live cells, as they take up AO stain. Those cells which were yellowish-orange represent apoptotic cells as they have compromised membranes that absorb EB stain. AO in dead cells dominates over EB stain thus, giving orange color. Necrotic cells are stained red with disintegrated membranes.

In the co-infection model, we observed, the percentage of necrotic cells was increased significantly as moved from single infection to co-infection. This staining provides a hint that when co-infection occurs, major percentage of cells undergo necrosis. This might be due to pathogen burden in co-infected cells as compared to single infected/transfected cells. Hence, it was understood, as previously suggested by expression profile of apoptotic and anti-apoptotic markers, that co-infection of SARS-CoV-2 and *H. pylori* in colon cells might show necrosis, rather than apoptosis.

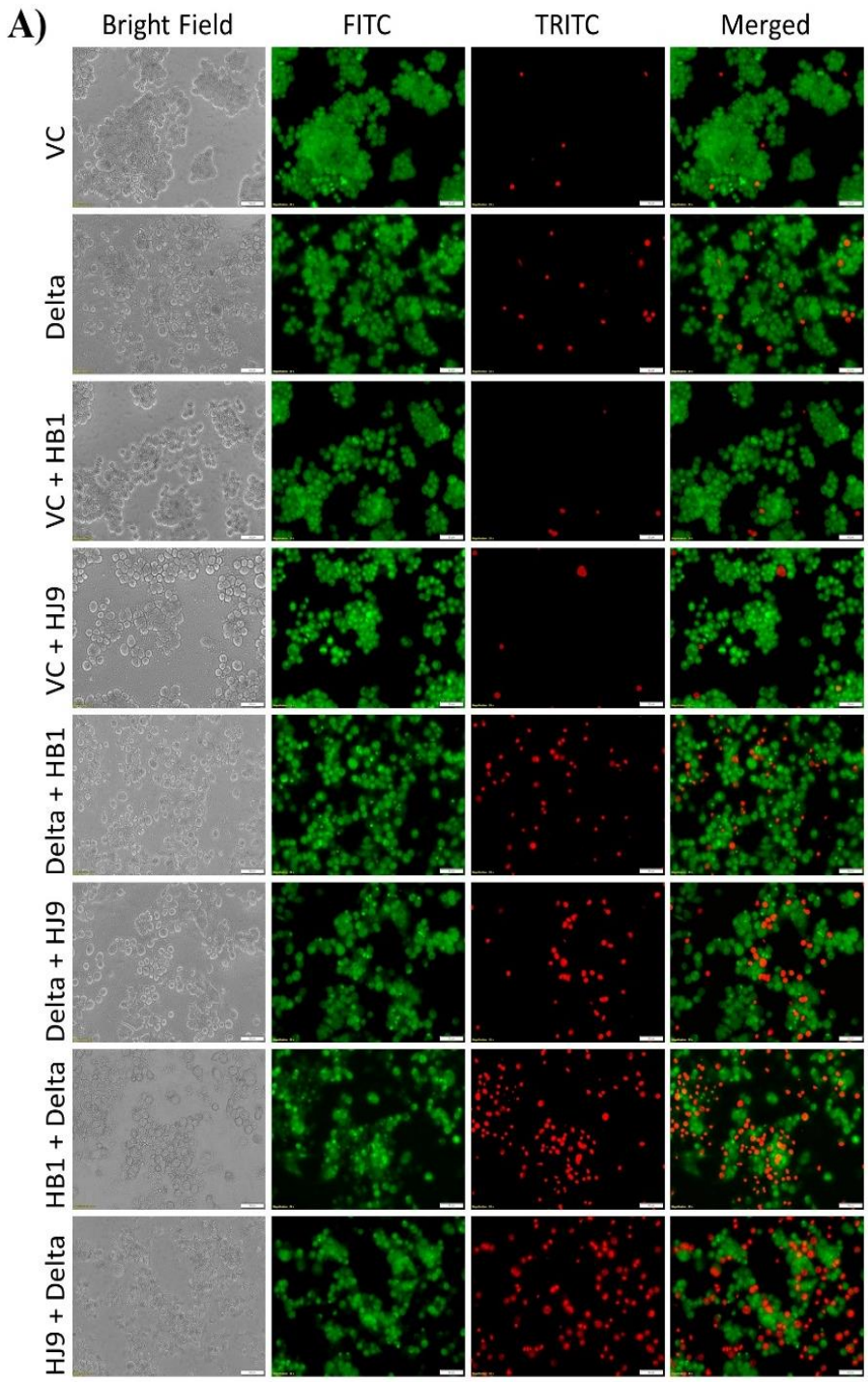
A)
Bright Field
FITC
TRITC
Merged
VC
Delta
VC + HB1
VC + HJ9
Delta + HB1
Delta + HJ9
HB1 + Delta
HJ9 + Delta

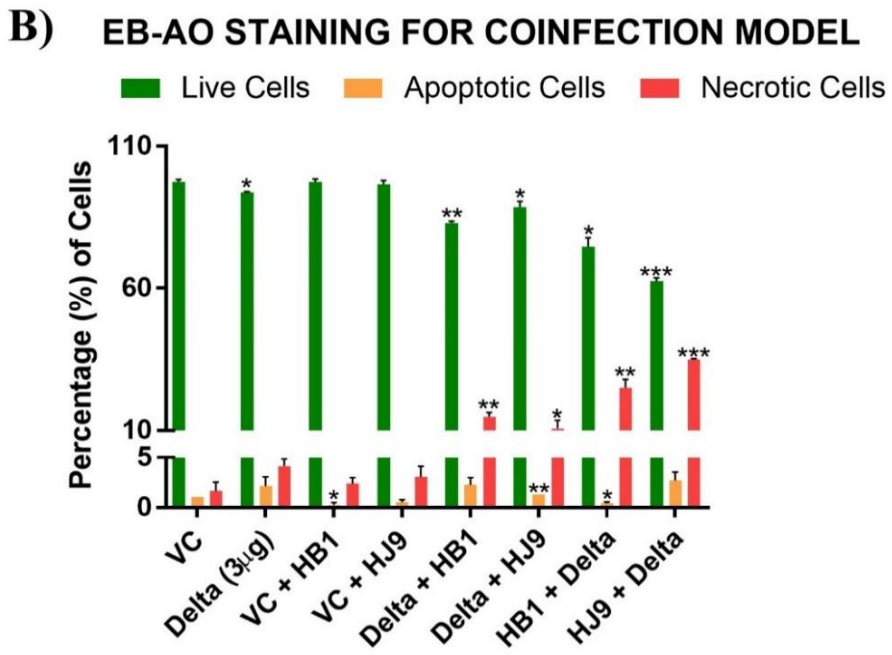

Figure 5.14 **Cell Death study in co-infection model through EB/AO staining.** A) Dual acridine orange and ethidium bromide staining of HT-29 cells infected according to the co-infection model signifies various modes of programmed cell death. B) Quantification of EB/AO-stained HT-29 cells were performed using Image J software. The significance test was calculated taking Vector Control (VC) as reference. p-values of <0.05, <0.01 and < 0.001 were considered statistically significant and represented with *, ** and ***, respectively.

5.4.4 Necroptosis study in co-infection model

Since, EB/AO staining and qRT- PCR of apoptotic genes suggested a necroptotic mode of cell death. To validate this result further, we checked the expression of necrosis marker at protein level. One such necrotic marker is RIP1. It is an adaptor kinase commonly involved in necrosis and apoptosis pathway.

As found out by previous experiments, we observed the elevated expression of RIP1 in *H. pylori* and SARS-CoV-2 co-infected samples, as compared to bacteria-only infected sample or Delta-only transfected sample.

Studies have reported that, RIP1 kinase undergoes autophosphorylation in TNFα-induced necroptosis. This phosphorylation activates RIP1 and helps it to recruit RIP3, thus forming a necrosome complex [60]. As previously found out by our study, that TNFα is significantly upregulated at transcript level, in *H. pylori* + SARS-CoV-2 infected samples. Hence, this indicates that TNFα induced necrosis might be one of the major pathways involved at the time of co-infection.

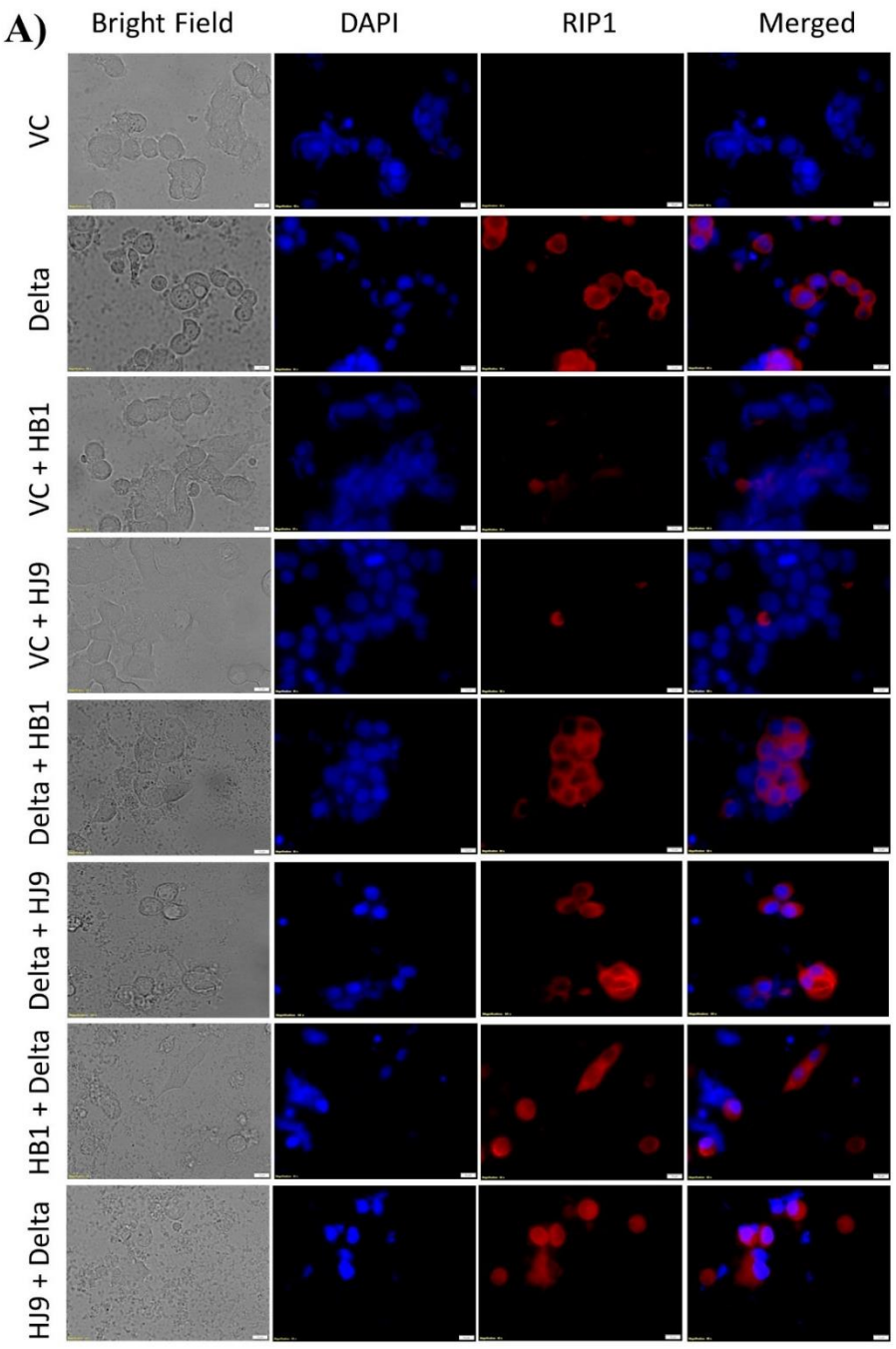
A)
Bright Field
DAPI
RIP1
Merged
VC
Delta
VC + HB1
VC + HJ9
Delta + HB1
Delta + HJ9
HB1 + Delta
HJ9 + Delta

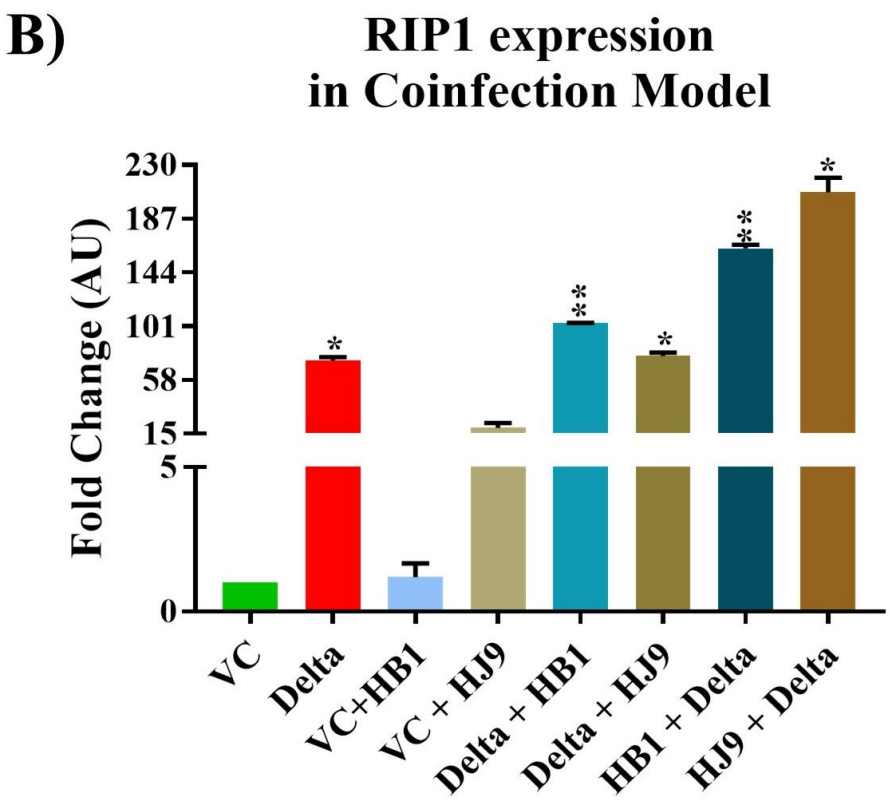

Figure 5.15 **Relative expression of RIP1 - Necroptotic marker in co-infection model.** A) Changes in the expression of RIP1 in HT-29 cells infected according to the co-infection model signifies level of necroptosis in each sample. B) Quantification was performed using Image J software. The significance test was calculated taking Vector Control (VC) as reference. p-values of <0.05, <0.01 and < 0.001 were considered statistically significant and represented with *, ** and ***, respectively.

CHAPTER 6: CONCLUSION AND SCOPE FOR FUTURE WORK

6.1 Conclusion

It has been established till now, that SARS-CoV-2 has receptors for cellular entry other than ACE2. But the molecular mechanism is yet to be elucidated. Our study is an effort to understand this mechanism in terms of gastrointestinal tract [61].

Through this co-infection study, we conclude that SARS-CoV-2 and *H. pylori* co-infection, in general, upregulate the release of inflammatory cytokines and chemokines, particularly IL-10, TNFα, CXCL1. Among these cytokines and chemokines, TNFα is the most reported in COVID-19 patients. Significant fold change in expression of TLR2 suggests that *H. pylori* and SARS-CoV-2 might support each other in infection as both the pathogens use TLR2 to induce their respective inflammatory pathway.

Further, our co-infection model i. e. infection of *H. pylori* followed by infection of SARS-CoV-2, mimics the natural scenario as human gut is pre-colonized with *H. pylori* and SARS-CoV-2 infection is the 2nd infection that occurs in gut. This makes our study more relevant.

Significant reduction in mitochondrial potential and mitochondrial mass clearly indicates that co-infection of *H. pylori* and SARS-CoV-2 causes mitochondrial damage. This might be probably due to high pathogenic load on cells. Similarly, in human gut when SARS-CoV-2 infects, pre-infected colon or gastric cells, cause pathogen burden. This induces cytokine storm and necroptotic death in cells.

As reported by our work, co-infection of *H. pylori* and SARS-CoV-2 induces inflammation through NF-κB pathway. This is one of the

inflammatory pathways that are commonly found to be upregulated in both bacterial and viral infections. NF-κB is reportedly activated by TNFα, which again was found to be upregulated in our co-infection model. This suggests that *H. pylori* and spike protein of SARS-CoV-2 might induce TNFα- NF-κB pathway, that further leads to the associated inflammatory response.

As further visualized by the cell death assay, necroptosis was reported in the co-infection model. The upregulation of RIP1, the necroptotic marker justifies the observed necroptosis in the co-infection model. It is intriguing to note that the RIP1 marker is also stimulated by TNFα, which triggers autophosphorylation.

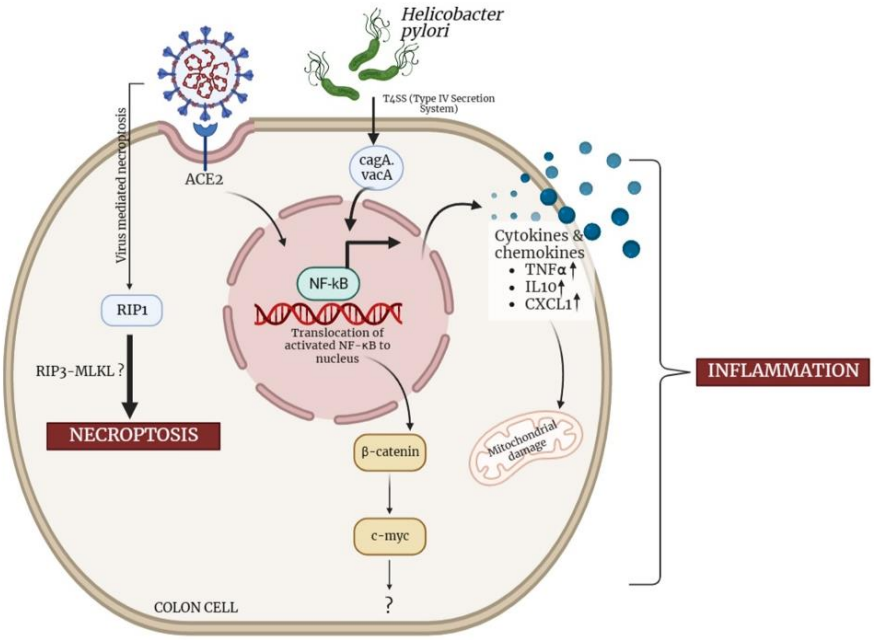

Figure 6.1 **A schematic diagram shows the probable mechanism by which *H. pylori* and SARS-CoV-2 co-infection induces inflammation and cell death in colon cells.**

6.2 Future Prospects

This study holds high significance in understanding the molecular mechanism behind co-infection-induced inflammation and cell death pathways. This further, will help in understanding which major pathways are involved in such cytokine storm in human body, which further transcends to gastrointestinal symptoms in COVID-19 patients. Moreover, our study provides a possible mechanistic understanding of SARS-CoV-2 and other bacterial co-infections in the gut microenvironment by understanding its effect on inflammation and cell death. To further decipher the detailed mechanism of cell death and mitochondrial damage, necroptotic proteins like RIP3, MLKL, mitochondrial genes like cytochrome c and ROS associated genes like NADH oxidase, malate dehydrogenase can be studied.

In the same co-infection model, Raman spectroscopy and LC-MS can be performed to check other molecules involved in inflammation and necroptosis due to co-infection in colon cells. This will give a deeper understanding of pathways studied under this thesis.

Once, the pathways are better understood, various phytochemicals commonly found in ‘Kadha’, an Indian traditional drink, can be tested on co-infection model. This will help understand if such phytochemicals can reduce the necrosis and inflammation associated with already studied pathways. One such phytochemical, piperin, an alkaloid found in Black pepper has strong binding affinity with the spike protein of nCoV-19. Similarly, Ursolic acid, phytochemical found in Tulsi, one of the ingredients of ‘kadha’ also shows high binding affinity for spike protein. Study involving the effect of ‘kadha’ in mitigating the gastrointestinal manifestations of SARS-CoV-2 can be beneficial to society.

ANNEXURES

Table 3: List of Primers used for qRT-PCR

S. N.	GENES	NCBI reference ID	Primer Sequence
1	SARS-CoV-2 *spike (S)* glycoprotein	NC_045 512.2	F: ACAGGCACAGGTGTTCTTAC R: GATCACGGACAGCATCAGTAG
2	*il-6* (Interleukin 6)	BC0155 11	F: TACCCCCAGGAGAAGATTCC R: TTTTCTGCCAGTGCCTCTTT
4	*il-1ß* (Interleukin - 1 beta)	NM_000 572	F: TGCCTTCAGCAGAGTGAAGA R: GGTCTTGGTTCTCAGCTTGG
6	*ifn-ß1*	NM_002 176.3	F: ACTGCCTCAAGGACAGGATG R: AGCCAGGAGGTTCTCAACAA
7	*ifn-ß2*	BC0155 11	F: TACCCCCAGGAGAAGATTCC R: TTTTCTGCCAGTGCCTCTTT
8	*cxcl1* (C-X-C motif chemokine ligand 1)	BC0119 76	F: AGGGAATTCACCCCAAGAAC R: TGGATTTGTCACTGTTCAGCA
9	*ifn-γ* (Interferon Gamma)	NM_000 619.2	F: TGACCAGAGCATCCAAAAGA R: CTCTTCGACCTCGAAACAGC
10	*tnfα* (Tumor Necrosis Factor alpha)	M10988. 1	F: CAGAGGGCCTGTACCTCATC R: GGAAGACCCCTCCCAGATAG
11	*tlr2*	AB4456 24.1	F: TGATGCTGCCATTCTCATTC R: CGCAGCTCTCAGATTTACCC

12	*apaf-1* (Apoptotic peptidase activating factor 1)	NM_181861.2	F: CTTGCTGCCCTTCTCCATGA R: TTGCGAAGCATCAGAATGCG
13	*fadd*	NC_000011.10	F: CACCAAGATCGACAGCATCG R: AGATTCTCAGTGACTCCCGC
14	*bid* (BH3 interacting domain death agonist)	NM_001196.4	F: CTGCAGGCCTACCCTAGAGA R: GTGTGACTGGCCACCTTCTT
15	*bak*	NC_000006.12	F: GGTTTTCCGCAGCTACGTTT R: AGCGTCGGTTGATGTCGTC
16	*bax* (Bcl_2 associated X)	NM_001291428.2	F: CATGGGCTGGACATTGGACT R: AAAGATGGTCACGGTCTGCC
17	*bcl_2* (apoptosis regulator)	NM_000633.2	F: CATGTGTGTGGAGAGCGTCA R: CATGTAAAGCCAGCCTCCGT
18	*caspase 9*	NC_000001.11	F: TGCTCAGACCAGAGATTCGC R: TCTTTCTGCTCGACATCACCAA
19	*gapdh* (Glyceraldehyde-3-Phosphate Dehydrogenase)	NG_009342.4	F: TGCACCACCAACTGCTTAG R: GATGCAGGGATGATGTTC

Table 4: List of Antibodies used for western blot/ immuno-fluorescence experiments

S.N.	ANTIBODY	Reference Number	Dilution	Protein band size (M.W.) in kDa
1	SARS-CoV-2 Spike protein	E7V3M	1:50, IF	100, 220
2	NF-κB p65	D14E12	1:1000, WB	65
3	ß-catenin	D10A8	1:1000, WB	92
4	Caspase 8	ABM14C1	1:1000, WB	43, 12/10
5	Caspase 3	5A1E	1:1000, WB	19, 17
6	RIP1	D94C12	1:250, IF	78

REFERENCES

[1] A. A. Al-Qahtani, "Severe Acute Respiratory Syndrome Coronavirus 2 (SARS-CoV-2): Emergence, history, basic and clinical aspects," *Saudi Journal of Biological Sciences*, vol. 27, no. 10, pp. 2531–2538, Oct. 2020, doi: 10.1016/j.sjbs.2020.04.033.

[2] "WHO Coronavirus (COVID-19) Dashboard." https://covid19.who.int (accessed May 03, 2023).

[3] Q. Zhang *et al.*, "Molecular mechanism of interaction between SARS-CoV-2 and host cells and interventional therapy," *Signal Transduction and Targeted Therapy*, vol. 6, no. 1, 2021. doi:10.1038/s41392-021-00653-w

[4] S. Belouzard, J. K. Millet, B. N. Licitra, and G. R. Whittaker, "Mechanisms of Coronavirus Cell Entry Mediated by the Viral Spike Protein," *Viruses*, vol. 4, no. 6, pp. 1011–1033, Jun. 2012, doi: 10.3390/v4061011.

[5] C. B. Jackson, M. Farzan, B. Chen, and H. Choe, "Mechanisms of SARS-CoV-2 entry into cells," *Nature Reviews Molecular Cell Biology*, vol. 23, no. 1, pp. 3–20, 2021. doi:10.1038/s41580-021-00418-x

[6] J. Machhi *et al.*, "The Natural History, Pathobiology, and Clinical Manifestations of SARS-CoV-2 Infections," *J Neuroimmune Pharmacol*, vol. 15, no. 3, pp. 359–386, 2020, doi: 10.1007/s11481-020-09944-5.

[7] W. T. Harvey *et al.*, "SARS-CoV-2 variants, spike mutations and immune escape," *Nat Rev Microbiol*, vol. 19, no. 7, Art. no. 7, Jul. 2021, doi: 10.1038/s41579-021-00573-0.

[8] G. McLean *et al.*, "The impact of evolving SARS-CoV-2 mutations and variants on COVID-19 vaccines," *mBio*, vol. 13, no. 2, 2022. doi:10.1128/mbio.02979-21

[9] F. Salamanna, M. Maglio, M. P. Landini, and M. Fini, “Body Localization of ACE-2: On the Trail of the Keyhole of SARS-CoV-2,” *Frontiers in Medicine*, vol. 7, 2020, doi: 10.3389/fmed.2020.594495.

[10] R. Ilikci Sagkan and D. F. Akin-Bali, “Structural variations and expression profiles of the SARS-CoV-2 host invasion genes in lung cancer,” *J Med Virol*, vol. 92, no. 11, pp. 2637–2647, Nov. 2020, doi: 10.1002/jmv.26107.

[11] J. Troisi, G. Venutolo, M. Pujolassos Tanyà, M. Delli Carri, A. Landolfi, and A. Fasano, “COVID-19 and the gastrointestinal tract: Source of infection or merely a target of the inflammatory process following SARS-CoV-2 infection?,” *World J Gastroenterol*, vol. 27, no. 14, pp. 1406–1418, Apr. 2021, doi: 10.3748/wjg.v27.i14.1406.

[12] A. Groff *et al.*, “Gastrointestinal Manifestations of COVID-19: A Review of What We Know,” *Ochsner J*, vol. 21, no. 2, pp. 177–180, 2021, doi: 10.31486/toj.20.0086.

[13] N. Sukharani *et al.*, “Gastrointestinal Manifestation of COVID-19 in Hospitalized Patients,” *Cureus*, vol. 13, no. 9, p. e18024, doi: 10.7759/cureus.18024.

[14] Y. Chen *et al.*, “The presence of SARS-CoV-2 RNA in the feces of COVID-19 patients,” *J Med Virol*, vol. 92, no. 7, pp. 833–840, Jul. 2020, doi: 10.1002/jmv.25825.

[15] P. Petakh *et al.*, “Immunoregulatory Intestinal Microbiota and COVID-19 in Patients with Type Two Diabetes: A Double-Edged Sword,” *Viruses*, vol. 14, no. 3, p. 477, Feb. 2022, doi: 10.3390/v14030477.

[1] A. A. Al-Qahtani, “Severe Acute Respiratory Syndrome Coronavirus 2 (SARS-CoV-2): Emergence, history, basic and clinical aspects,” *Saudi Journal of Biological Sciences*, vol. 27, no. 10, pp. 2531–2538, Oct. 2020, doi: 10.1016/j.sjbs.2020.04.033.

[2] “WHO Coronavirus (COVID-19) Dashboard.” https://covid19.who.int (accessed May 03, 2023).

[3] Q. Zhang *et al.*, “Molecular mechanism of interaction between SARS-CoV-2 and host cells and interventional therapy,” *Signal Transduction and Targeted Therapy*, vol. 6, no. 1, 2021. doi:10.1038/s41392-021-00653-w

[4] S. Belouzard, J. K. Millet, B. N. Licitra, and G. R. Whittaker, “Mechanisms of Coronavirus Cell Entry Mediated by the Viral Spike Protein,” *Viruses*, vol. 4, no. 6, pp. 1011–1033, Jun. 2012, doi: 10.3390/v4061011.

[5] C. B. Jackson, M. Farzan, B. Chen, and H. Choe, “Mechanisms of SARS-CoV-2 entry into cells,” *Nature Reviews Molecular Cell Biology*, vol. 23, no. 1, pp. 3–20, 2021. doi:10.1038/s41580-021-00418-x

[6] J. Machhi *et al.*, “The Natural History, Pathobiology, and Clinical Manifestations of SARS-CoV-2 Infections,” *J Neuroimmune Pharmacol*, vol. 15, no. 3, pp. 359–386, 2020, doi: 10.1007/s11481-020-09944-5.

[7] W. T. Harvey *et al.*, “SARS-CoV-2 variants, spike mutations and immune escape,” *Nat Rev Microbiol*, vol. 19, no. 7, Art. no. 7, Jul. 2021, doi: 10.1038/s41579-021-00573-0.

[8] G. McLean *et al.*, “The impact of evolving SARS-CoV-2 mutations and variants on COVID-19 vaccines,” *mBio*, vol. 13, no. 2, 2022. doi:10.1128/mbio.02979-21

[9] F. Salamanna, M. Maglio, M. P. Landini, and M. Fini, “Body Localization of ACE-2: On the Trail of the Keyhole of SARS-CoV-2,” *Frontiers in Medicine*, vol. 7, 2020, doi: 10.3389/fmed.2020.594495.

[10] R. Ilikci Sagkan and D. F. Akin-Bali, “Structural variations and expression profiles of the SARS-CoV-2 host invasion genes in lung

cancer," *J Med Virol*, vol. 92, no. 11, pp. 2637–2647, Nov. 2020, doi: 10.1002/jmv.26107.

[11] J. Troisi, G. Venutolo, M. Pujolassos Tanyà, M. Delli Carri, A. Landolfi, and A. Fasano, "COVID-19 and the gastrointestinal tract: Source of infection or merely a target of the inflammatory process following SARS-CoV-2 infection?," *World J Gastroenterol*, vol. 27, no. 14, pp. 1406–1418, Apr. 2021, doi: 10.3748/wjg.v27.i14.1406.

[12] A. Groff *et al.*, "Gastrointestinal Manifestations of COVID-19: A Review of What We Know," *Ochsner J*, vol. 21, no. 2, pp. 177–180, 2021, doi: 10.31486/toj.20.0086.

[13] N. Sukharani *et al.*, "Gastrointestinal Manifestation of COVID-19 in Hospitalized Patients," *Cureus*, vol. 13, no. 9, p. e18024, doi: 10.7759/cureus.18024.

[14] Y. Chen *et al.*, "The presence of SARS-CoV-2 RNA in the feces of COVID-19 patients," *J Med Virol*, vol. 92, no. 7, pp. 833–840, Jul. 2020, doi: 10.1002/jmv.25825.

[15] P. Petakh *et al.*, "Immunoregulatory Intestinal Microbiota and COVID-19 in Patients with Type Two Diabetes: A Double-Edged Sword," *Viruses*, vol. 14, no. 3, p. 477, Feb. 2022, doi: 10.3390/v14030477.

[16] L. Bernard-Raichon *et al.*, "Gut microbiome dysbiosis in antibiotic-treated COVID-19 patients is associated with microbial translocation and bacteremia," *Nat Commun*, vol. 13, no. 1, Art. no. 1, Nov. 2022, doi: 10.1038/s41467-022-33395-6.

[17] H. Zhang *et al.*, "Specific ACE2 expression in small intestinal enterocytes may cause gastrointestinal symptoms and injury after 2019-nCoV infection," *Int J Infect Dis*, vol. 96, pp. 19–24, Jul. 2020, doi: 10.1016/j.ijid.2020.04.027.

[18] N. Balamtekin, C. Artuk, M. Arslan, and M. Gülşen, "The Effect of *Helicobacter pylori* on the Presentation and Clinical Course of Coronavirus Disease 2019 Infection," *J Pediatr Gastroenterol Nutr*,

vol. 72, no. 4, pp. 511–513, Apr. 2021, doi: 10.1097/MPG.0000000000003005.

[19] Y. Liu et al., “Roles of the gut microbiota in severe SARS-CoV-2 infection,” *Cytokine & Growth Factor Reviews*, vol. 63, pp. 98–107, 2022. doi:10.1016/j.cytogfr.2022.01.007

[20] B. A. Salih, “*Helicobacter pylori* Infection in Developing Countries: The Burden for How Long?,” *Saudi J Gastroenterol*, vol. 15, no. 3, pp. 201–207, Jul. 2009, doi: 10.4103/1319-3767.54743.

[21] L. E. Wroblewski, R. M. Peek, and K. T. Wilson, “*helicobacter pylori* and gastric cancer: Factors that modulate disease risk,” *Clinical Microbiology* Reviews, vol. 23, no. 4, pp. 713–739, 2010. doi:10.1128/cmr.00011-10

[22] S. Kumar, G. K. Patel, and U. C. Ghoshal, “*Helicobacter pylori*-Induced Inflammation: Possible Factors Modulating the Risk of Gastric Cancer,” *Pathogens*, vol. 10, no. 9, p. 1099, Aug. 2021, doi: 10.3390/pathogens10091099.

[23] D. Bravo, A. Hoare, C. Soto, M. A. Valenzuela, and A. F. Quest, “*Helicobacter pylori* in human health and disease: Mechanisms for local gastric and systemic effects,” *World J Gastroenterol*, vol. 24, no. 28, pp. 3071–3089, Jul. 2018, doi: 10.3748/wjg.v24.i28.3071.

[24] Y. Moodley et al., “Age of the association between *helicobacter pylori* and man,” *PLoS Pathogens*, vol. 8, no. 5, 2012. doi:10.1371/journal.ppat.1002693

[25] X.-W. Wu, H.-Z. Ji, M.-F. Yang, L. Wu, and F.-Y. Wang, “*Helicobacter pylori* infection and inflammatory bowel disease in Asians: A meta-analysis,” *World J Gastroenterol*, vol. 21, no. 15, pp. 4750–4756, Apr. 2015, doi: 10.3748/wjg.v21.i15.4750.

[26] R. M. Delahay and M. Rugge, “Pathogenesis of *helicobacter pylori* infection,” *Helicobacter*, vol. 17, pp. 9–15, 2012. doi:10.1111/j.1523-5378.2012.00976.x

[27] Y. Yu, S. Zhu, P. Li, L. Min, and S. Zhang, "*Helicobacter pylori* infection and inflammatory bowel disease: a crosstalk between upper and lower digestive tract," *Cell Death Dis*, vol. 9, no. 10, Art. no. 10, Sep. 2018, doi: 10.1038/s41419-018-0982-2.

[28] B. W. Massey, K. Jayathilake, and H. Y. Meltzer, "Respiratory microbial co-infection With SARS-CoV-2," *Frontiers in Microbiology*, vol. 11, 2020, https://www.frontiersin.org/articles/10.3389/fmicb.2020.02079

[29] S. Khan, M. S. Shafiei, C. Longoria, J. W. Schoggins, R. C. Savani, and H. Zaki, "SARS-CoV-2 spike protein induces inflammation via TLR2-dependent activation of the NF-κB pathway," *eLife*, vol. 10, p. e68563, Dec. 2021, doi: 10.7554/eLife.68563.

[30] S. M. Smith, "Role of toll-like receptors in *helicobacter pylori* infection and immunity," *World Journal of Gastrointestinal Pathophysiology*, vol. 5, no. 3, p. 133, 2014. doi:10.4291/wjgp.v5.i3.133

[31] C. Peng, Y. Ouyang, N. Lu, and N. Li, "The NF-κB Signaling Pathway, the Microbiota, and Gastrointestinal Tumorigenesis: Recent Advances," *Front. Immunol.*, vol. 11, p. 1387, Jun. 2020, doi: 10.3389/fimmu.2020.01387.

[32] H. Islam, T. C. Chamberlain, A. L. Mui, and J. P. Little, "Elevated Interleukin-10 Levels in COVID-19: Potentiation of Pro-Inflammatory responses or impaired anti-Inflammatory action?," *Frontiers in Immunology*, vol. 12, 2021, https://www.frontiersin.org/articles/10.3389/fimmu.2021.677008

[33] S. Villapol, "Gastrointestinal symptoms associated with COVID-19: impact on the gut microbiome," *Transl Res*, vol. 226, pp. 57–69, Dec. 2020, doi: 10.1016/j.trsl.2020.08.004.

[34] M. Morais da Silva et al., "Cell death mechanisms involved in cell injury caused by sars-cov-2," *Reviews in Medical Virology*, vol. 32, no. 3, 2021. doi:10.1002/rmv.2292

[35] S. Li *et al.*, “SARS-CoV-2 triggers inflammatory responses and cell death through caspase-8 activation,” *Sig Transduct Target Ther*, vol. 5, no. 1, Art. no. 1, Oct. 2020, doi: 10.1038/s41392-020-00334-0.

[36] J. N. Gustine and D. Jones, “Immunopathology of Hyperinflammation in COVID-19,” *Am J Pathol*, vol. 191, no. 1, pp. 4–17, Jan. 2021, doi: 10.1016/j.ajpath.2020.08.009.

[37] S. Piplani, P. K. Singh, D. A. Winkler, and N. Petrovsky, “In silico comparison of SARS-CoV-2 spike protein-ace2 binding affinities across species and implications for virus origin,” *Scientific Reports*, vol. 11, no. 1, 2021. doi:10.1038/s41598-021-92388-5

[38] M. A. Kelliher, S. Grimm, Y. Ishida, F. Kuo, B. Z. Stanger, and P. Leder, “The death domain kinase RIP mediates the TNF-induced NF-κB signal,” *Immunity*, vol. 8, no. 3, pp. 297–303, Mar. 1998, doi: 10.1016/S1074-7613(00)80535-X.

[39] R. Kircheis et al., “NF-κB pathway as a potential target for treatment of critical stage COVID-19 patients,” *Frontiers in Immunology*, vol. 11, 2020. doi:10.3389/fimmu.2020.598444

[40] S. D. Tyrkalska, A. Martínez-López, A. Pedoto, S. Candel, M. L. Cayuela, and V. Mulero, “The Spike protein of SARS-CoV-2 signals via Tlr2 in zebrafish,” *Developmental & Comparative Immunology*, vol. 140, p. 104626, Mar. 2023, doi: 10.1016/j.dci.2022.104626.

[41] Y. Jiang *et al.*, “Inflammatory pathways in Covid-19: Mechanism and therapeutic interventions,” *MedComm*, vol. 3, no. 3, 2022. doi:10.1002/mco2.154

[42] C.-Y. Lee et al., “Tumor necrosis factor-alpha exacerbates viral entry in sars-cov2-infected IPSC-derived cardiomyocytes,” *International Journal of Molecular Sciences*, vol. 22, no. 18, p. 9869, 2021. doi:10.3390/ijms22189869

[43] E. Varfolomeev, T. Goncharov, and D. Vucic, “Immunoblot analysis of the regulation of TNF receptor family-induced NF-κB signaling by

C-IAP proteins," *Methods in Molecular Biology*, pp. 109–123, 2021. doi:10.1007/978-1-0716-1669-7_7

[44] Y. Guo *et al.*, "Targeting TNF-α for COVID-19: Recent Advanced and Controversies," *Front Public Health*, vol. 10, p. 833967, Feb. 2022, doi: 10.3389/fpubh.2022.833967.

[45] S. Bhaskar et al., "Cytokine storm in covid-19—immunopathological mechanisms, clinical considerations, and therapeutic approaches: The reprogram consortium position paper," *Frontiers in Immunology*, vol. 11, 2020. doi:10.3389/fimmu.2020.01648

[46] Tang, Y., Liu, J., Zhang, D., Xu, Z., Ji, J., & Wen, C. (2020). "Cytokine Storm in COVID-19: The Current Evidence and Treatment Strategies." *Frontiers in Immunology*, 11. https://doi.org/10.3389/fimmu.2020.01708

[47] Howell, M. C., Green, R., McGill, A. R., Dutta, R., Mohapatra, S., & Mohapatra, S. S. (2021). "SARS-CoV-2-Induced Gut Microbiome Dysbiosis: Implications for Colorectal Cancer." *Cancers*, *13*(11), 2676. https://doi.org/10.3390/cancers13112676

[48] K. Hilpert and R. Mikut, "Is there a connection between gut microbiome dysbiosis occurring in COVID-19 patients and post-covid-19 symptoms?," *Frontiers in Microbiology*, vol. 12, 2021. doi:10.3389/fmicb.2021.732838

[49] C. Ferreira, S. D. Viana, and F. Reis, "Gut Microbiota Dysbiosis–Immune Hyperresponse–Inflammation Triad in Coronavirus Disease 2019 (COVID-19): Impact of Pharmacological and Nutraceutical Approaches," *Microorganisms*, vol. 8, no. 10, Art. no. 10, Oct. 2020, doi: 10.3390/microorganisms8101514.

[50] Jia, H. P., Look, D. C., Shi, L., Hickey, M., Pewe, L., Netland, J., Farzan, M., Wohlford-Lenane, C., Perlman, S., & McCray, P. B. (2005). ACE2 Receptor Expression and Severe Acute Respiratory Syndrome Coronavirus Infection Depend on Differentiation of Human Airway

[51] Ni, W., Yang, X., Yang, D., Bao, J., Li, R., Xiao, Y., Hou, C., Wang, H., Liu, J., Yang, D., Xu, Y., Cao, Z., & Gao, Z. (2020). Role of angiotensin-converting enzyme 2 (ACE2) in COVID-19. Critical Care, 24(1). https://doi.org/10.1186/s13054-020-03120-0

[52] Peek, R. M., & Blaser, M. J. (2002). *Helicobacter pylori* and gastrointestinal tract adenocarcinomas. Nature Reviews Cancer, 2(1), 28–37. https://doi.org/10.1038/nrc703

[53] A. Lamb and L.-F. Chen, "Role of the *Helicobacter pylori*-induced inflammatory response in the development of gastric cancer," J Cell Biochem, vol. 114, no. 3, pp. 491–497, Mar. 2013, doi: 10.1002/jcb.24389.

[54] Díaz, P., Valenzuela Valderrama, M., Bravo, J., & Quest, A. F. G. (2018). *Helicobacter pylori* and Gastric Cancer: Adaptive Cellular Mechanisms Involved in Disease Progression. Frontiers in Microbiology, 9. https://doi.org/10.3389/fmicb.2018.00005

[55] Maubach, G., Vieth, M., Boccellato, F., & Naumann, M. (2022). *Helicobacter pylori*-induced NF-κB: trailblazer for gastric pathophysiology. Trends in Molecular Medicine, 28(3), 210–222. https://doi.org/10.1016/j.molmed.2021.12.005

[56] D. C. Rio, M. Ares, G. J. Hannon, and T. W. Nilsen, "Purification of RNA using TRIzol (TRI reagent)," Cold Spring Harb Protoc, vol. 2010, no. 6, p. pdb.prot5439, Jun. 2010, doi: 10.1101/pdb.prot5439.

[57] D. Kashyap et al., "*Helicobacter pylori* infected gastric epithelial cells bypass cell death pathway through the oncoprotein Gankyrin," Advances in Cancer Biology - Metastasis, vol. 7, p. 100087, Jul. 2023, doi: 10.1016/j.adcanc.2023.100087.

[58] D. C. Rio, M. Ares, G. J. Hannon, and T. W. Nilsen, “Purification of RNA using TRIzol (TRI reagent),” Cold Spring Harb Protoc, vol. 2010, no. 6, p. pdb.prot5439, Jun. 2010, doi: 10.1101/pdb.prot5439.

[59] D. Kashyap et al., “Oral rinses in growth inhibition and treatment of *Helicobacter pylori* infection,” BMC Microbiol, vol. 20, p. 45, Mar. 2020, doi: 10.1186/s12866-020-01728-4.

[60] Festjens, N., Vanden Berghe, T., Cornelis, S., & Vandenabeele, P. (2007). “RIP1, a kinase on the crossroads of a cell's decision to live or die.” Cell Death & Differentiation, 14(3), 400–410. https://doi.org/10.1038/sj.cdd.4402085

[61] Sonkar, C., Kashyap, D., Varshney, N., Baral, B., & Jha, H. C. (2020). “Impact of Gastrointestinal Symptoms in COVID-19: a Molecular Approach.” *SN Comprehensive Clinical Medicine*, 2(12), 2658–2669. https://doi.org/10.1007/s42399-020-00619-z